THE JOURNAL OF COMPARATIVE NEUROLOGY 249:337-357 (1986)

Anatomy and Physiology of Saccadic Burst Neurons in the Alert Squirrel Monkey. I. Excitatory Burst Neurons

A. STRASSMAN, S.M. HIGHSTEIN, AND R.A. McCREA
Department of Neuroscience, The Albert Einstein College of Medicine, New York, New York 10461

ABSTRACT

Saccadic burst neurons in the pontine reticular formation have been implicated in the generation of saccades in the horizontal plane on the basis of lesion and extracellular recording studies in the cat and monkey. In the present study, saccadic burst neurons were anatomically and physiologically characterized with intraaxonal recording and injection of horseradish peroxidase in the alert squirrel monkey. A population of burst neurons were found that appear analogous to the excitatory burst neurons (EBNs) described previously in the cat. All neurons are located in the caudal pontine reticular formation and have a major axonal projection to the ipsilateral abducens nucleus. Additional projections were found to the medial vestibular nucleus, the nucleus prepositus, and regions of the pontine and medullary reticular formation rostral, ventral, and caudal to the abducens. All neurons fire exclusively during saccades and have a discharge pattern similar to that of medium-lead burst neurons described previously in the cat and monkey. In most neurons the saccadic burst begins 5–15 msec before saccade onset. Linear relationships exist between burst duration and saccade duration, number of spikes in the burst and saccade amplitude, and firing frequency and instantaneous velocity. Physiological activity of each neuron shows the closest relationship with the amplitude of the saccade component in a particular direction. For all neurons, this on-direction is in the ipsilateral hemifield and is predominantly horizontal, but may have either an upward or downward vertical component. These results support a major role for the EBNs in the monkey in generating the saccadic burst in abducens motoneurons, as well as in contributing to the oculomotor activity in other classes of premotor neurons.

Key words: saccade, eye movement, oculomotor, reticular formation, vestibular

Proper vision is dependent upon the precise control of eye movements. Different types of eye movements serve to direct the eyes toward a desired visual target as well as to hold the eyes steady with respect to the target, even during head or target movements. Saccades are the finely controlled rapid movements that redirect the eyes toward a new visual target (Dodge, '03; Yarbus, '67; Carpenter, '77). They are generated by a high-frequency burst of firing in extraocular muscle motoneurons (Robinson, '70; Schiller, '70; Fuchs and Luschei, '70; Henn and Cohen, '73; Goldstein, '83) that produces an abrupt rise in muscle tension and moves the eye rapidly against the viscosity of the orbital tissues to its new position (Robinson et al., '69; Collins et al., '75). At the end of the saccade, motoneuron firing frequency falls to the level required for holding the eye in its new position against the elastic restoring forces of the orbital tissues. Motoneurons innervating the antagonist muscles behave in a reciprocal manner, exhibiting a pause in firing during the saccade, followed by a rise to a firing frequency appropriate for the new position of fixation.

Of the six extraocular muscles moving each eye, the medial and lateral recti are primarily responsible for eye movements in the horizontal plane. The abducens nucleus

Accepted January 29, 1986.

S.M. Highstein's present address is the Department of Otolaryngology, Washington University School of Medicine, St. Louis, MO 63110.

R.A. McCrea's present address is the Committee on Neurobiology Department of Pharmacological and Physiological Sciences, University of Chicago, Chicago, IL 60637.

Address reprint requests to A. Strassman at his present address, Neurology Service, Massachusetts General Hospital, Boston, MA 02114.

contains both the motoneurons that innervate the lateral rectus muscle and the internuclear neurons that project to motoneurons in the oculomotor nucleus innervating the medial rectus muscle (Graybiel and Hartweig, '74; Highstein and Baker, '78; Steiger and Büttner-Ennever, '78, '79; Highstein et al., '82). The internuclear neurons have a motoneuronlike discharge during eye movements (Delgado-Garcia et al., '77; McCrea et al., '86a) that is relayed with high synaptic efficacy to the medial rectus motoneurons (Highstein and Baker, '78). Thus, horizontal conjugate eye movement is controlled almost entirely by the abducens nucleus.

Lesion and stimulation studies in the monkey have identified the paramedian pontine reticular formation as being critically involved in the generation of horizontal rapid eye movements (Cohen et al., '68; Cohen and Komatsuzaki, '72). Extracellular tracer studies in both the cat and monkey show projections to the ipsilateral abducens nucleus from this region of the reticular formation, as well as a crossed projection to the contralateral abducens nucleus from the region of the reticular formation ventral and caudal to the abducens (Büttner-Ennever and Henn, '76; Graybiel, '77; Maciewicz et al., '77; Gacek, '79).

Studies of unit activity during eye movements in the cat and monkey have identified a class of neurons in these regions of the reticular formation that fire a high-frequency burst of action potentials for saccades and are otherwise silent (Sparks and Travis, '71; Cohen and Henn, '72; Luschei and Fuchs, '72; Keller, '74; Henn and Cohen, '76; van Gisbergen et al., '81; Kaneko et al., '81; Yoshida et al., '82). The timing and intensity of the discharge of these saccadic burst neurons are appropriate for producing the saccadic modulation in the motoneurons. In both the burst neuron and the motoneuron, the duration of the saccadic burst is approximately equal to saccade duration, while the number of spikes in the burst is related to the amplitude of the ipsilateral component of the movement.

Burst neurons in the reticular formation caudal to the abducens have been thoroughly characterized in the cat with electrophysiological and anatomical techniques and have been found to exert an inhibitory synaptic action on contralateral abducens motoneurons (Hikosaka and Kawakami, '77; Hikosaka et al., '78). These inhibitory burst neurons (IBNs) also have crossed projections to the vestibular nuclei, the nucleus prepositus hypoglossi, and the pontomedullary reticular formation (Hikosaka et al., '80; Yoshida et al., '82)

Anatomical and electrophysiological characteristics of burst neurons in the reticular formation rostral to the abducens are less well documented. Orthodromic microstimulation studies in the cat indicate an excitatory synaptic action of these neurons on ipsilateral abducens motoneurons (Igusa et al., '80), while antidromic microstimulation demonstrates axonal branching of these excitatory burst neurons (EBNs) in the ipsilateral abducens nucleus, as well as in the medial vestibular nucleus and the medullary reticular formation (Sasaki and Shimazu, '81).

The similar organization of reticular projections to the abducens in the monkey as compared with that in the cat (Büttner-Ennever and Henn, '76; Graybiel, '77) suggests there may be a similar synaptic organization of burst neuron input to motoneurons in the two species. However, direct electrophysiological and anatomical demonstrations of burst neuron projections to the abducens exist only in the cat.

The recently developed technique of intraaxonal injection of HRP in the alert animal (McCrea et al., '80; Yoshida et al., '82; McCrea et al., '86a,b) provides a highly detailed view of the soma location and axonal projections of behaviorally identified neurons, allowing a more precise and reliable description of the functional anatomy of premotor pathways than is possible with extracellular recording and labelling techniques. In the present study, this technique is used to determine burst neuron soma locations and axonal projections in the squirrel monkey. These data are critical for confirming a reciprocal organization of burst neuron input to the abducens in the monkey comparable to that found in the cat. In addition, identification of the regions outside of the abducens receiving burst neuron projections is important for consideration of premotor brainstem saccadic mechanisms. Neurons with a saccadic modulation of firing superimposed on a steady discharge proportional to eye position have been found in the vestibular nuclei and the nucleus propositus, which project heavily to the abducens. Burst neurons, by way of collateral projections, are candidates for generating the saccadic burst or pause in these neurons.

Knowledge of burst neuron projections is particularly important in evaluating the possible role of burst neurons in generating the eye position signal of the motoneuron. It has been suggested that the burst neuron's velocity signal, in addition to being relayed directly to the motoneuron, is fed into a neural integrator that converts it to the eye position signal also required by the motoneuron (Robinson, '71, '75). Although the location of the integrator is not known, this model implies that it receives a projection from burst neurons. A precise localization of burst neuron projections, particularly to brainstem regions carrying an eye position signal, might be relevant to considerations of the location and organization of the neural integrator.

This paper reports the anatomical and physiological characteristics of EBNs in the squirrel monkey; IBNs are described in the following paper (Strassman et al., '86).

METHODS

Surgical preparation

Adult male squirrel monkeys (650–900 g) were surgically prepared for recording in two stages under sterile operating conditions. They were anesthetized by sodium pentobarbital (Nembutal), initial dose of 25 mg/kg i.p., supplemented by additional i.m. administration as needed to maintain deep surgical anesthesia. Ampicillin (Omnipen, 50 mg/day i.m.) was given postoperatively. In the first stage a stainless-steel bolt was cemented to the occipital bone to allow painless immobilization of the head, and a Teflon-coated wire coil (10.5-mm diameter) was implanted on the sclera of one eye (adapted from Judge et al., '80) for measurement of eye position (Robinson, '63; see below). For implantation of the bolt, the animal's head was held in a stereotaxic frame, while the bolt was held by a frame-mounted manipulator. The same clamp that held the bolt to the manipulator during implantation was also used to hold the bolt for immobilization of the animal's head in the chair during recording. This method of implantation ensured that the monkey's head was held in a consistent orientation within the field coils during recording, without any tilt about the

naso-occipital (roll) axis. During recording the monkey's head was pitched 20° nose down with respect to the stereotaxic plane; this pitch angle brings the horizontal semicircular canals nearly parallel to earth horizontal and approximates the animal's natural resting head orientation.

After recovery from the first surgery, the monkeys were placed for 1–2 hours/day in the primate chair used for recording. Their heads were fixed by the implanted bolt, but their body and limbs were free to move. After 2 weeks, the monkeys were anesthetized as described above and the second stage of surgery was performed. A posterior craniotomy was performed, and a section of posterior parietal cortex on one side was removed by aspiration to expose the tentorium cerebelli. A hollow Mylar recording chamber was implanted with one open end (4 × 5 mm) in contact with the tentorium, and the other end (8 × 9 mm) was fixed to the skull with dental acrylic. The tentorium at the bottom of the chamber was then removed to expose the cerebellar surface. The recording chamber was filled with sterile bone wax and sealed with a Plexiglas cap. During and after surgery cerebral edema was controlled with dexamethasone (2–5 mg/kg per day, i.m.). Monkeys were usually alert and active within 12–24 hours following this surgical procedure and showed no obvious sensory or motor deficits. To determine whether they showed an unrestricted and symmetrical range of eye movements, a storage oscilloscope was used to create an X-Y display of eye position during several minutes of spontaneous eye movements. For all animals used in these experiments, the storage display showed a horizontally and vertically symmetrical field of movement, with an overall range of approximately 30° horizontally and 40° vertically.

Recording

Horizontal and vertical eye movements were measured with the scleral search coil technique (Robinson, '63), in which the monkey was placed with his head in the center of two orthogonal magnetic fields generated by two orthogonal pairs of two-foot-diameter magnetic field coils, and eye position was obtained by sampling the current induced in the implanted scleral coil.The system could resolve movements of less than 0.5° and was linear for rotations of 20° in each direction. Eye movement calibration was carried out by rotating the field coils around the anesthetized monkey and was confirmed by measurement of the gain of the vestibulo-ocular reflex of the alert monkey in the light. In addition, it was determined that the signal generated by field coil rotation about a stationary test coil differed in amplitude from the signal generated by an equal rotation of the test coil by not more than 5%.

Neuronal activity was recorded with glass micropipettes pulled from 3 mm glass tubing, bevelled to a tip diameter of 0.5–1.0 μm, and filled with a 10% solution of HRP in 0.05 M Tris buffer (pH 7.3) and 0.5 M KCl; electrode resistances were 25–35 MΩ. A micromanipulator was used to drive the electrodes through the cerebellum and the IVth ventricle into the brainstem, with the electrodes angled 10° medially and 26° rostrally with respect to the stereotaxic plane. Passage of the electrode through the cerebellum was marked by recordings from Purkinje cells, with their characteristic complex spike activity. Entrance of the electrode into the IVth ventricle was marked by a complete silencing of all recorded neuronal activity. Tracks through the abducens nucleus were characterized by somatic recordings from large numbers of neurons with an ipsilateral burst tonic firing pattern; tracks through the medial longitudinal fasciculus (MLF) encountered axons in large numbers with burst tonic or tonic-vestibular-pause firing patterns (King et al., '76; Pola and Robinson, '78). Electrode tracks were made primarily in a region between 1 mm caudal and 1 mm rostral to the abducens nuclei, and up to 2 mm lateral on both sides of the midline. AC-coupled recordings of neuronal discharge during spontaneous saccades were stored on magnetic analog tape with simultaneously recorded horizontal and vertical eye position for subsequent analysis.

Burst neurons were identified by their exclusively saccade-related firing pattern. They were usually impaled axonally in the dorsal reticular formation immediately ventral to the abducens nucleus or the MLF, 1–2 mm ventral to the IVth ventricle (the morphological evidence for the identification of injection sites is described below). The absence of injury discharge was demonstrated by the neurons' silence during periods of fixation. In some cases, neuronal firing could be recorded extracellularly prior to the intracellular impalement; in such cases, additional firing during saccades was recorded intracellularly prior to labelling to verify the firing pattern of the impaled neuron.

Neurons were labelled with HRP by passage of depolarizing current through the recording electrode in 250–500 msec, 10–nA pulses, 50% duty cycle, for as long as the intracellular penetration could be maintained, usually 1–4 minutes. Resting potential during intraaxonal recordings (monitored with a DC-coupled oscilloscope trace) was typically 25–50 mV prior to current injection. Current injection was briefly interrupted every 20–30 seconds to record additional neuronal activity during saccades and verify that the neuron displayed the same saccadic discharge pattern as had been observed prior to the injection. Current injection was terminated when the cell was lost or the resting potential dropped below 20mV.

The tip of a 26=gauge needle cemented to the skull at the edge of the recording chamber provided an arbitrary reference point for measuring the relative mediolateral, rostrocaudal, and dorsoventral coordinates of every electrode track and injection site. The coordinates of the IVth ventricle, the surface of the brainstem, the abducens nucleus, the MLF, and the genu of the VII nerve (identified by the presence of axons that fire exclusively during blinks) were also noted when these anatomical landmarks were encountered during a track, and so could be used subsequently in the histological identification of tracks and injection sites. Usually not more than one injection was attempted per track. In three cases, two neurons were injected on a single track, with a distance of more than 1 mm separating the two injection sites. Eight to 12 injections were usually attempted in a 12-hour period.

Histological preparation

Twenty-four hours after the first injection, the monkey was anesthetized with pentobarbital, injected intravenously with 1,000 units of Heparin and 0.5 cc of 0.2 M sodium nitrite, and perfused transcardially with 500 cc of 0.9% saline followed by 1.5 liters of 0.7% paraformaldehyde and 1.3% glutaraldehyde in 0.05 M phosphate buffer, pH 7.4. The brain was blocked in the plane of the electrode tracks, and the brainstem and cerebellum were placed in

25% sucrose in phosphate buffer. After the tissue sank, 80-μm coronal frozen sections were cut and incubated according to a modification of the nickel-cobalt-intensified diaminobenzidine (DAB) reaction of Adams ('81). Sections were preincubated at room temperature for 20 minutes in a solution of 0.05% DAB, 0.025% cobalt chloride, and 0.02% nickel ammonium sulfate in 0.05 M phosphate buffer, pH 6.7 (pH of solution after addition of DAB was 6.4), and then incubated in the dark at room temperature in the presence of hydrogen peroxide for 45–60 minutes. Sections were mounted, dehydrated, cleared, and coverslipped.

Identification of injection sites

The sections were examined to locate all evidence of electrode tracks and injection sites present in the tissue. Because the tissue was cut in the plane of the electrode tracks, the tracks could be located by the presence of blood cells forming a dorsoventrally oriented line through the cerebellum and into the dorsal part of the brainstem. The location at which a stained axon had been injected could be identified by a number of characteristic signs, including an increased intensity of staining; the presence of aberrant morphological features such as gross swelling (see Fig. 9B of Strassman et al., '86), fragmentation, or degeneration; and the presence of stained glia. The location of the tracks and injection sites relative to each other, and with respect to anatomical landmarks, was used to match each stained neuron with the corresponding neuronal activity recorded when the neuron was injected.

Physiological analysis

Neuronal firing and eye position channels on the tape were digitized and analyzed with a PDP 11/73 computer. The digitized horizontal and vertical eye position traces were displayed on a screen along with the digitized spike data. The beginning and end of each saccade was marked by eye with the aid of a crosshair, and the saccade and associated burst, if any, were included in the analysis. Regression analyses were performed between saccade duration and burst duration, saccade amplitude and the number of spikes in the burst, and instantaneous velocity and instantaneous frequency. Latency from burst onset to saccade onset was also measured.

An analysis was carried out to determine whether the firing of a neuron during a saccade was related to the amplitude of the component of the saccade in a specific direction (the on-direction for that neuron) (similar to the methods of Henn and Cohen, '76; and Kaneko et al., '81). A regression analysis was carried out for each neuron to determine the correlation coefficient and slope (in spikes/degree) relating the number of spikes in each saccadic burst with the amplitude of the component of the saccade in a given direction ("rcos(theta)," where r is the amplitude of the saccade and theta is the direction of the saccade with respect to an arbitrary reference direction). This regression analysis was performed for every reference direction between 0° and 359°, varying the reference direction in 1° steps. For each neuron, the two directions were found for which the regression analysis yielded the highest correlation coefficient and the highest slope.

Figure 1 illustrates this procedure for one EBN, whose activity was recorded during 46 spontaneous saccades. (This neuron is anatomically illustrated in Fig. 16B.) In Figure 1A–D, the number of spikes in a saccadic burst is plotted

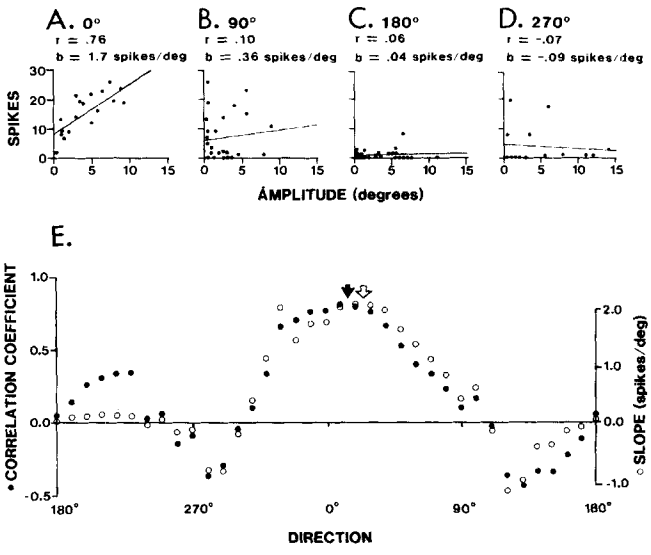

Fig. 1. Determination of on-direction. A–D. Plots of the number of spikes in the burst (ordinate) versus the amplitude of the saccade in a given direction (abscissa) for four directions (0°,90°,180° ,270°). r = correlation coefficient, b = slope. A total of 46 saccades are included in these plots; for each plot, only saccades within 90° of the direction being tested are shown. E. Plot of correlation coefficient (filled circles) and slope (open circles) on the ordinate, versus the reference direction on the abscissa, for the same neuron as in A–D. The filled and open arrowheads indicate the directions with the highest correlation coefficient and slope, respectively.

on the ordinate versus amplitude of the saccade component in a given direction on the abscissa, for four different directions (0°, 90°, 180°, 270°, where 0° = ipsilateral, 90° = up). The linear regression line relating the two variables is shown for each plot. Each regression analysis included only those saccades with a positive component in the direction being tested (saccades whose directions were within 90° of the reference direction, so that cos(theta) > 0); saccades with a negative component in each direction were tested separately (as in Fig. 1A,C). Each regression analysis required a minimum of three points, or at least three saccades within 90° of the reference direction being tested. Thus, completion of the on-direction analysis, with testing of all 360 reference directions, requires a sample of saccades distributed in all directions.

The firing of the neuron illustrated in Figure 1 shows a much higher correlation coefficient (.76) and slope (1.7 spikes/degree) in relation to the ipsilateral component of the saccade (1A) than in relation to the upward (1B), downward (1D), or contralateral (1C) component of the saccade.

Figure 1E shows a plot of the correlation coefficient (filled circles) and slope (open circles) on the ordinate versus the reference direction used for the regression analysis on the abscissa. The filled arrowhead indicates the direction with the highest correlation coefficient (15°; correlation coefficient = .81, slope = 2.1 spikes/degree); the open arrowhead indicates the direction with the highest slope (25°; correlation coefficient = .79, slope = 2.2 spikes/degree). The slope and correlation coefficient are thus similar for these two directions. The slope was considered the most direct measure of neuronal sensitivity, but the validity of this measurement was considered to depend on the strength of the associated correlation. For this reason, the direction with the largest slope was chosen as the on-direction if the cor-

relation coefficient in that direction was within .08 of the maximum correlation coefficient (this was the case for 75% of the neurons); otherwise, the direction with the maximum correlation coefficient was used. Using these criteria, 25° was chosen as the on-direction for the neuron shown in Figure 1. Using either slope or correlation coefficient as the criteria for on-direction gives a similar distribution of on-directions for the population as a whole.

An on-direction was calculated for every neuron. The accuracy of the on-direction determination depends on the number of saccades recorded for the neuron. The description of on-direction characteristics in the Results (Fig.4) is based on 17 EBNs, for which an average of 57 saccades were recorded per neuron. The five remaining EBNs were each recorded during 10–20 saccades and were not included in Figure 4. One of these neurons was also excluded from Figure 5.

Anatomical analysis

Stained neurons were reconstructed with the aid of a microscope and drawing tube. Background staining from endogenous peroxidase activity was adequate for visualization of most cytoarchitectural borders. Camera lucida reconstructions were made of somatodendritic and axonal arborizations. Cross-sectional areas of somata and boutons were measured by drawing them on mm graph paper at a magnification of 1,500 × using a 100× oil immersion objective and a drawing tube, and counting the number of enclosed square mm boxes. Axonal diameters were determined from the mean of measurements made at several different sites along each axon, distal to the initial segment. The number of cells that give rise to particular collaterals or projections is reported as a percentage of the total number of cells that were judged to be sufficiently well stained at the site of collateralization.

Figure 17 is intended as a qualitative summary of the EBN projection sites. Such a coronal series was first plotted for each neuron by marking the location of each cluster of boutons (typically containing 10–30 boutons) with a dot. These individual plots were then combined to produce the population summary of Figure 17.

Two aspects of the experimental design maximized information concerning axonal projections at the expense of dendritic morphology: First, injections were made intraaxonally rather than intrasomatically, which results in more nearly complete axonal filling but is often inadequate for substantial dendritic filling; second, survival times following injections were as long as 26 hours, which maximizes axonal filling but also results in partial gliosis and degeneration of dendrites in many cases (unpublished observations). The resulting data is optimal for describing axonal projections, but largely inadequate for a thorough description of the fine morphological detail of dendrites. However, for a number of neurons the dendritic filling is adequate for a description of dendritic orientation and branching pattern.

Extracellular labelling

In several independent experiments, in order to retrogradely label neurons afferent to the abducens nucleus, a small extracellular injection of HRP was made iontophoretically into the left abducens nucleus (Fig.8). The injection was made by passing 1 μA of depolarizing current, 90% duty cycle, for 20 minutes through a glass micropipette (tip diameter = 15 μm) filled with a 10% solution of HRP in Tris-buffered 0.05 M KCl, pH 7.2. Following a 24-hour survival, the monkeys were anesthetized and perfused with a solution of 1% glutaraldehyde and 1% paraformaldehyde in 0.1 M phosphate buffer, pH 7.4. Frozen sections were cut and reacted with tetramethylbenzidine (TMB) (Mesulam, '78). Locations of retrogradely labelled cells were plotted and soma diameters were measured by using a camera lucida.

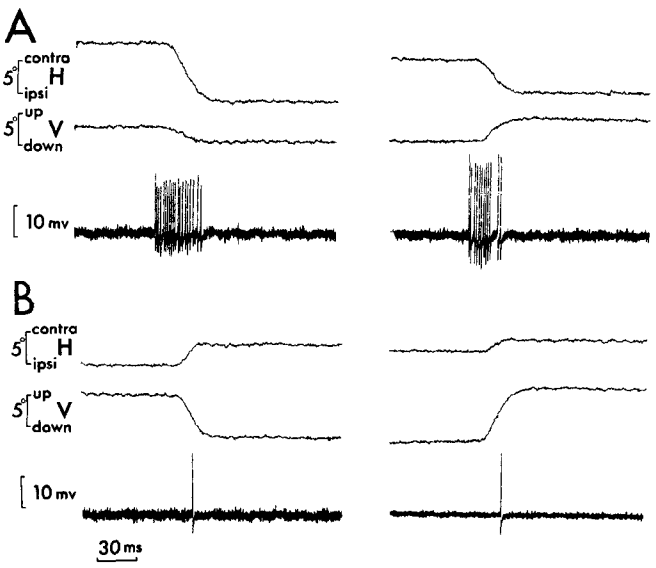

Fig. 2. Excitatory burst neuron (EBN) discharge during saccadic eye movements. Each of the panels in A and B shows horizontal eye position, vertical eye position, and intraaxonal recording of membrane potential. Voltage calibration of 10 mV applies to all records except the right panel in B, for which the calibration is 20 mV. A. Ipsilateral saccades. B. Contralateral saccades.

RESULTS

This report describes 22 neurons physiologically identified as saccadic burst neurons by their firing pattern during spontaneous saccades and anatomically identified on the basis of intracellular staining that was in every case adequate for visualization of both the soma location and the axonal projection to the abducens nucleus. The burst neurons described in this report are classified as EBNs on the basis of their soma location in the pontine reticular formation rostral to the abducens nucleus and their ipsilateral projection to the abducens (Igusa et al., '80; Sasaki and Shimazu, '81).

Physiology

The neurons in this study have a firing pattern similar to that of medium-lead burst neurons described previously (Cohen and Henn, '72; Luschei and Fuchs, '72; Keller, '74; van Gisbergen et al., '81; Kaneko et al., '81). All the neurons burst during saccades and are otherwise silent. For most neurons, the number of spikes in the burst depends on both the direction and the amplitude of the saccade. In addition, for all neurons the duration of the burst is linearly related to the duration of the saccade (see below).

Figure 2 illustrates the firing of an EBN during four spontaneous saccades. Two ipsilateral saccades (i.e., the

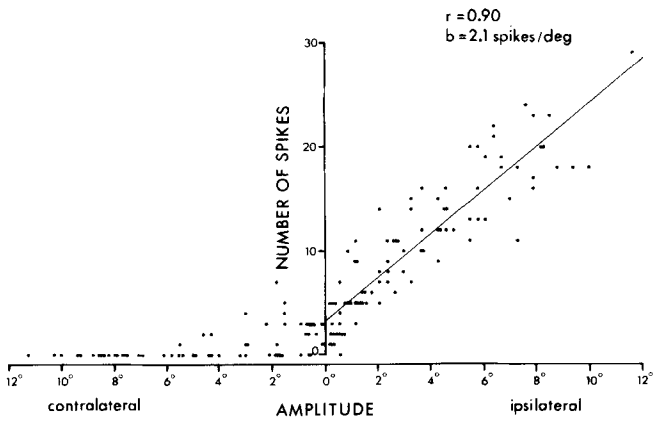

Fig. 3. Relationship between the number of spikes in the burst and the amplitude of the saccade in the on-direction, for the neuron shown in Figure 2. The number of spikes is plotted on the ordinate versus the amplitude of the on-direction component on the abscissa (i.e., rcos(theta); see Methods). The on-direction calculated for the neuron is 6° (not illustrated). The regression line was calculated by using only saccades with a component in the on-direction (i.e., using only points to the right of the ordinate).

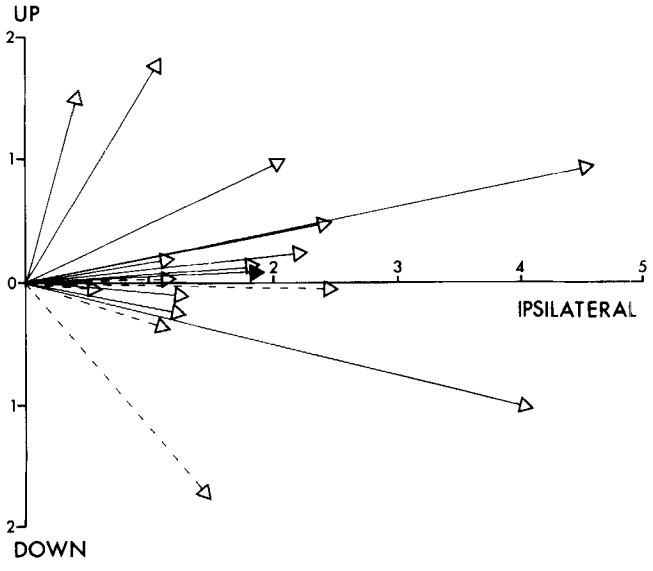

Fig. 4. Distribution of on-directions. Each neuron is represented in polar coordinates by a line and an arrowhead. The direction of each arrowhead shows the neuron's on-direction. The length of each line is proportional to the neuron's saccadic sensitivity in spikes/degree, as indicated by the scales on the horizontal and vertical axes (given by the slopes of the regression lines as shown in Fig. 3). Broken lines indicate neurons whose firing is related to direction of the saccade independent of amplitude (see text). The filled arrowhead indicates a neuron that projects to the trochlear and oculomotor nuclei.

saccades are directed to the left, and the neuron's soma is on the left side of the brain) are shown in Figure 2A and two contralateral saccades are shown in 2B. Figure 2A and 2B each show one saccade with a downward vertical component and one with an upward component. The neuron fires a burst of spikes beginning before the onset of ipsilateral saccades (Fig. 2A), and a smaller burst, here consisting of a single spike, occurring after the onset of contralateral saccades (Fig. 2B); the firing is unrelated to the vertical component of the saccade (see below). The neuron is silent during the periods of fixation preceding and following each saccade.

All of the neurons fire preferentially for saccades in a particular direction, described as the on-direction for that neuron (see Methods). Figure 3 shows a plot and regression line relating the number of spikes in the burst (ordinate) with the amplitude of the component of the saccade in the on-direction (abscissa), for the neuron illustrated in Figure 2. The on-direction calculated for this neuron is 6°. Only saccades with a component in the on-direction (the points to the right of the ordinate) were used in calculating the regression line. The regression line has a slope of 2.1 spikes/degree, and the correlation coefficient is 0.90. This neuron shows no significant correlation between the number of spikes in the burst and the amplitude of either the upward ($r = .07$) or downward ($r = -.06$) component of the saccade (not illustrated). For the entire sample of EBNs, the mean value of the slope relating neuronal firing to the amplitude of the on-direction component is 2.0 ± 1.0 spikes/degree; the mean correlation coefficient is 0.78 ± 0.12.

For the neuron in Figure 3, and for most of the EBNs, the regression line intercepts the ordinate at a positive value, indicating the presence of a burst during saccades perpendicular to the on-direction. The firing of most EBNs shows either no significant correlation (8/19, 42%) or a low negative correlation (10/19, 53%; $P < .05$) with the amplitude of the off-direction component of the saccade (off-direction = on-direction + 180°). For example, the neuron in Figure 3 has a correlation coefficient of -0.55 ($P < .001$, two-tailed) in relation to the off-direction amplitude; i.e., for the saccades plotted to the left of the ordinate, firing decreases with increasing saccade amplitude. One EBN shows a low positive correlation with the amplitude of the off-direction saccade component.

Figure 4 shows a polar plot of the distribution of on-directions for the EBNs. The direction of each arrowhead represents the neuron's on-direction, while the length of the arrow is proportional to the neuron's saccadic sensitivity (the scale is indicated along the horizontal and vertical axes in spikes/degree). As has been found in previous studies of burst neurons, the on-direction for every neuron is in the hemifield of movement ipsilateral to its soma, with a vertical component that may be either up or down. EBN on-directions are distributed symmetrically on either side of the horizontal axis; the mean on-direction for the population, either unweighted or weighted according to each neuron's slope, is not significantly different from 0°. 82% of the EBNs have on-directions within 30° of horizontal. The mean absolute value of the angle with horizontal (the angular distance, either up or down, from 0°) is 21°.

For most of the EBNs (71%), the number of spikes in the burst depends on both the direction and the amplitude of the saccade. However, for five EBNs (29%), the number of spikes in the burst has a higher correlation with cos(theta) than with rcos(theta) (r= amplitude, theta = direction of the saccade with respect to the on-direction), which indicates a relationship to saccade direction independent of amplitude. These five neurons are represented with broken lines in Figure 4.

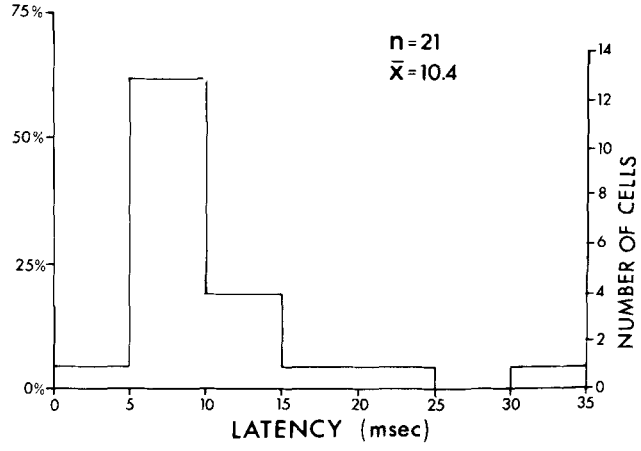

Fig. 5. Histogram of saccadic latency. Latency is defined as the interval between the first spike in the burst and the onset of the saccade.

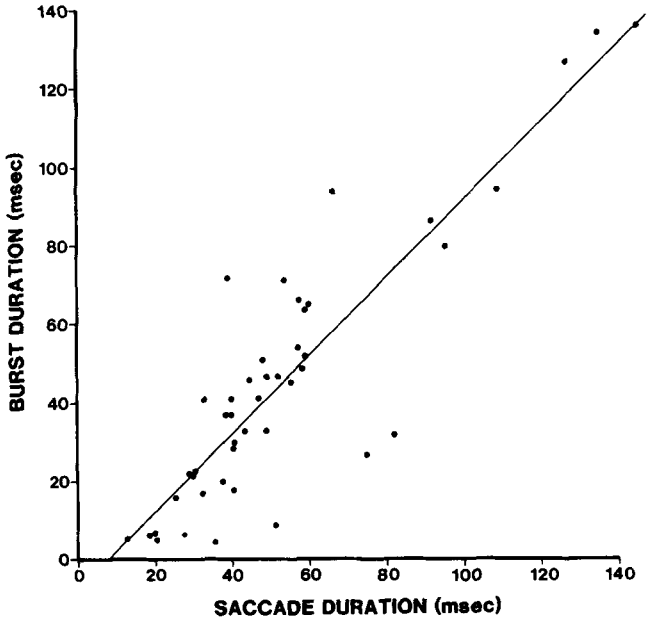

Fig. 6. Relationship between burst duration and saccade duration for one EBN. The slope of the regression line is 1.0; the correlation coefficient is .92.

Figure 5 is a histogram of the latency, or the time between burst onset and saccade onset, for the EBNs. As has been observed in previous studies of burst neurons (Cohen and Henn, '72; Luschei and Fuchs, '72; Keller, '74; van Gisbergen et al., '81; Kaneko et al., '81), the latency depends on the direction of the saccade, with ipsilateral and contralateral saccades having the longest- and shortest-lead bursts, respectively. This is true for most of the neurons, regardless of the on-direction. The values shown in Figure 5 are the mean latencies for saccades in the direction associated with the longest-lead bursts for each neuron.

The mean latency for the EBNs is 10.4 msec. Most of the EBNs have latencies between 5 and 15 msec. Three EBNs have longer latencies, between 15 and 32 msec; however, all of the neurons have firing characteristics typically associated with medium-lead burst neurons, including a high correlation between burst duration and saccade duration, an absence of any irregular discharge preceding the main burst, and, in most cases, a strong dependence of the number of spikes on amplitude as well as direction (Keller, '74; van Gisbergen et al., '81). In these respects, the three EBNs with longer latencies are distinguishable from most long-lead burst neurons found in the reticular formation (van Gisbergen et al., '81; Hepp and Henn, '83). In addition, the histogram of Figure 5 indicates a unimodal distribution and gives no clear basis for subdividing the population on the basis of latency.

Most of the neurons also show a significant correlation between instantaneous firing frequency and instantaneous eye velocity, although the correlations are in all cases lower than for the relation between the number of spikes and saccade amplitude. The mean slope for this relationship is 0.82 $\pm$ 0.82 spikes/second/degree/second; the mean correlation coefficient is .50 $\pm$ .19.

All of the neurons show a significant correlation between burst duration and saccade duration, with a mean correlation coefficient of .76 $\pm$ .18 and a mean slope of 1.14 $\pm$ 0.44. This relationship is illustrated for one EBN in Figure 6. The mean ratio of burst duration to saccade duration in the population is 1.18 $\pm$ 0.36.

Anatomy

Intraaxonal injection typically produced a diffuse backfilling of the soma and, in some cases, the proximal dendrites. In some cases in which the injection site was a greater distance from the soma, the diffuse filling extended in the retrograde direction only as far as the initial segment, and the soma was labelled by a granular reaction

Abbreviations

BC	brachium conjunctivum
BP	brachium pontis
CX	external cuneate nucleus
DVN	descending vestibular nucleus
INT	nucleus intercalatus
IO	inferior olive
LC	locus coeruleus
LVN	lateral vestibular nucleus
ML	medial lemniscus
MLF	medial longitudinal fasciculus
MVN	medial vestibular nucleus
NRTP	nucleus reticularis tegmenti pontis
P	pyramidal tract
PH	nucleus prepositus hypoglossi
PN	pontine nuclei
RB	restiform body
RF	reticular formation
RO	nucleus of Roller
SO	superior olive
SOL	nucleus of the solitary tract
SVN	superior vestibular nucleus
TB	trapezoid body
VLVN	ventral lateral vestibular nucleus
V PR	principal trigeminal nucleus
V SP	spinal trigeminal nucleus
VI	abducens nucleus
VI N	abducens nerve
VII	facial nucleus
VII N	facial nerve
X	dorsal motor nucleus of the vagus
XII	hypoglossal nucleus

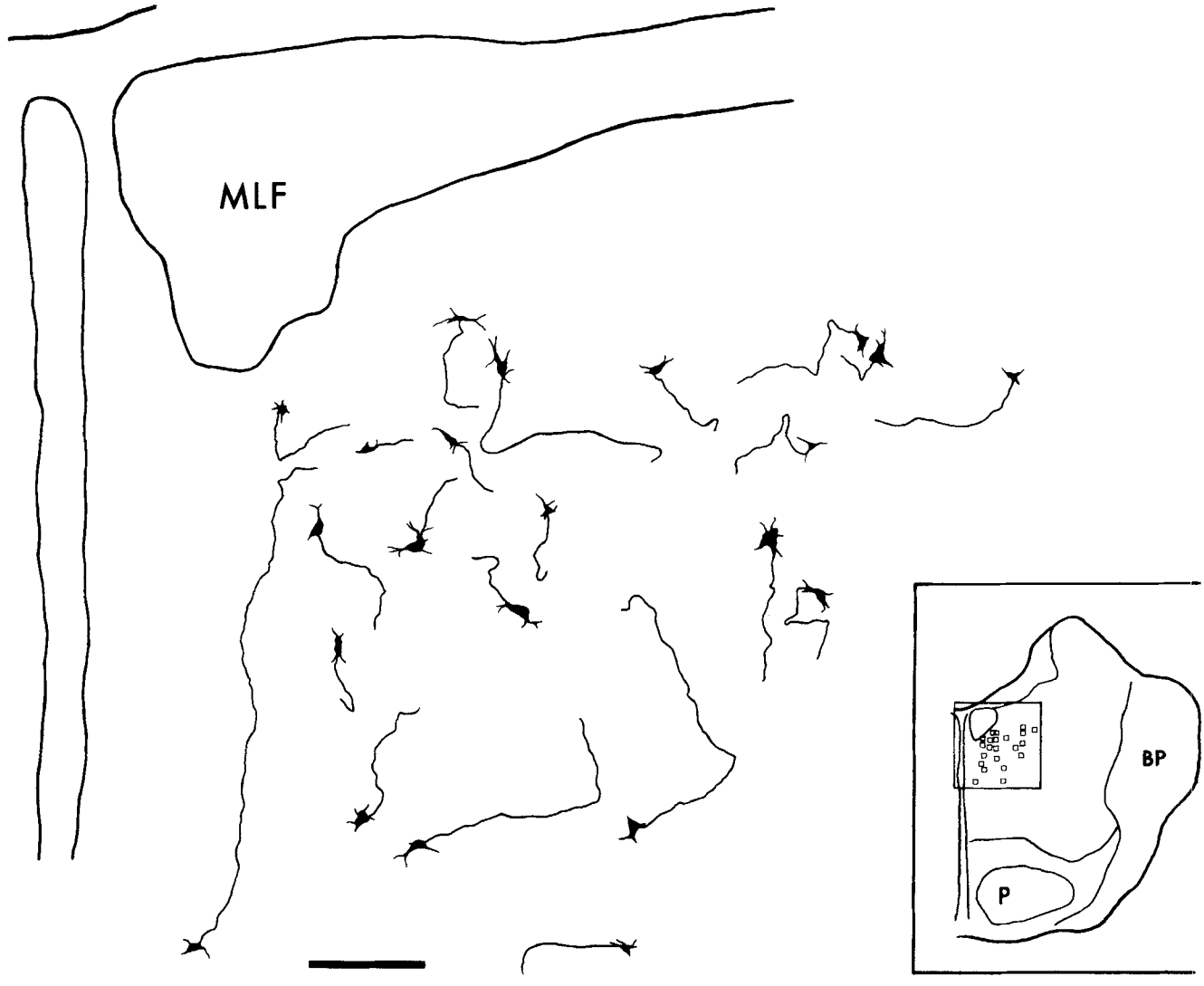

Fig. 7. Soma location and initial axonal trajectories of EBNs. EBNs are shown on a coronal section through the reticular formation rostral to the abducens. The inset shows the section at lower magnification, with the area containing the EBNs enclosed by a box in the dorsomedial reticular formation. The rostrocaudal level shown here included the levels shown in Figure 17A and B (cf. Fig.18C of Strassman et al., '86). Calibration = 200 μm.

product. Retrograde labelling of the soma (diffuse or granular) was the minimal requirement for including a burst neuron in this study.

Soma location

Figure 7 shows the somata and initial axonal trajectories of the EBNs on a coronal section through the caudal pons; the inset shows the section at lower magnification, with the region containing the burst neurons enclosed in a box in the dorsomedial reticular formation. The EBNs (n=22) are located in the dorsomedial part of the pontine reticular formation immediately rostral to the abducens, nucleus pontis centralis caudalis (Olszewski and Baxter, '54; Brodal, '57; Taber, '61). They occupy a region that extends 1 mm rostrally from the rostral border of the abducens, 0.4–1.5 mm from the midline, and 1–2.5 mm ventral to the IVth ventricle (also see Fig. 18C of Strassman et al., '86).

Figure 8 shows the distribution of retrogradely labelled neurons following a small extracellular injection of HRP in the left abducens nucleus. The distribution of neurons in the ipsilateral reticular formation rostral to the abducens (large dots in Fig. 8E–G) is similar in rostrocaudal, dorsoventral, and mediolateral extent to that of the EBNs shown in Figure 7. Additional labelled neurons are present in the contralateral medullary reticular formation (large dots in Fig. 8A–C), as well as in the vestibular nuclei, nucleus prepositus, and the ipsilateral medullary reticular formation (small dots in Fig. 8A–D).

Soma-dendritic and axonal morphology

Figure 9A shows a histogram of mean soma diameters for the EBNs. For comparison, Figure 9B shows the soma diameters of pontine reticular neurons that project ipsilaterally to the abducens (large dots in Fig. 8E–G). Mean

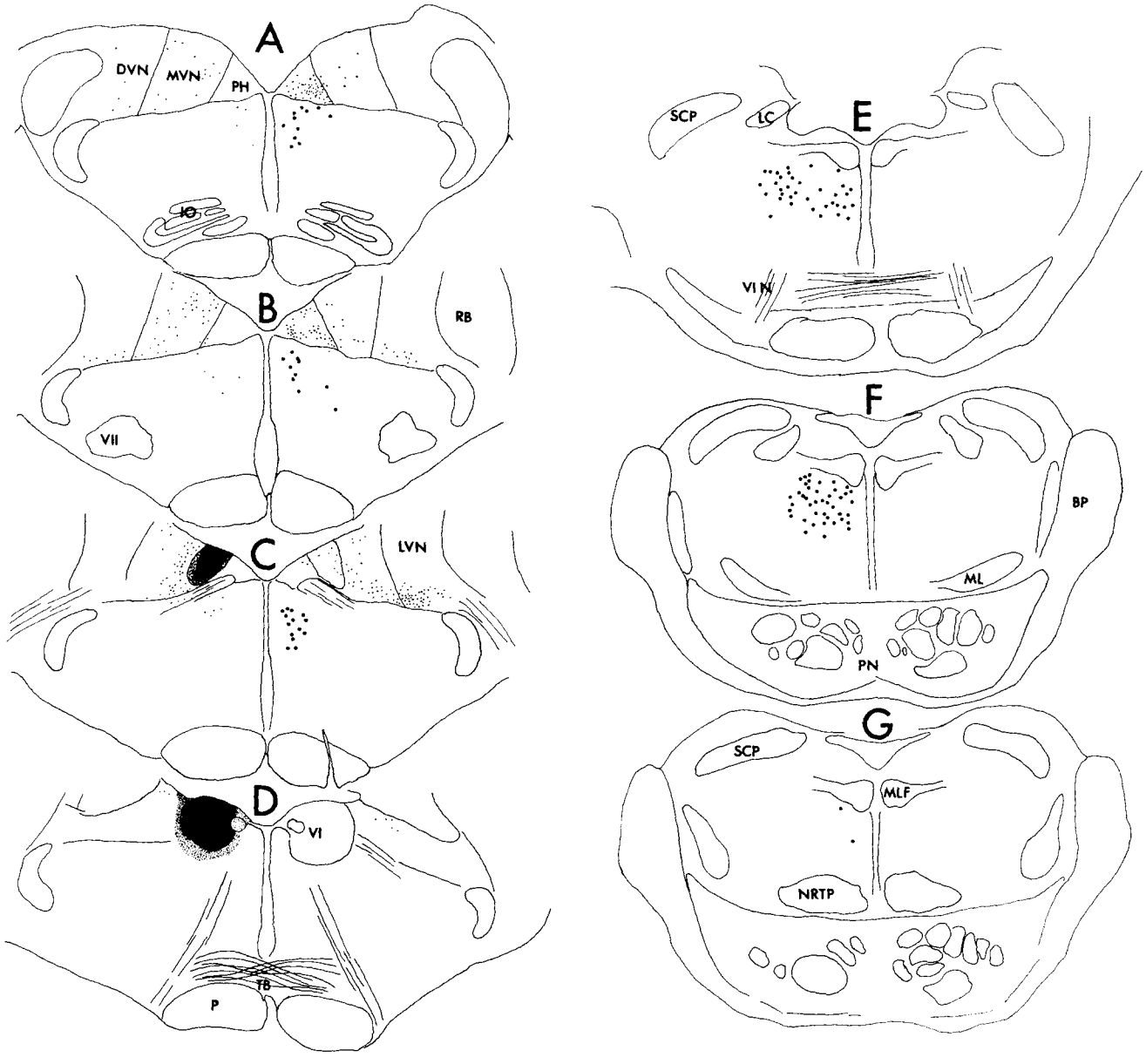

Fig. 8. Locations of retrogradely labelled cells following an extracellular injection of HRP in the left abducens nucleus. Large dots represent labelled cells in the ipsilateral pontine and contralateral medullary reticular formation; the soma diameters of these cells are compared with those of the EBNs and IBNs in Figure 9 and in Figure 8 of Strassman et al. ('86). Small dots represent labelled cells in other regions.

values for soma diameter are 22.7 ± 5.5 μm for EBNs and 18.0 ± 4.0 μm for the retrogradely labelled reticular neurons. Comparison of the two histograms in Figure 9 indicates a similar range of soma diameters, with a relatively lower proportion of smaller cells (10–20 μm) represented in the intracellularly labelled sample. The mean cross-sectional soma area for the EBNs is 387 ± 160 μm^2. No correlation was found between soma size and either burst latency or saccadic sensitivity (measured by using the slope of the regression line relating number of spikes to saccade amplitude, as well as the slope relating instantaneous firing frequency to instantaneous velocity).

Axon diameters of EBNs range from 1.7 to 4.7 μm (mean=3.1 ± 0.8); no correlation exists between soma size and axon diameter. Cross-sectional areas were measured for 324 axonal boutons, pooled from three EBNs; the mean bouton area is 1.01 ± 0.63 μm^2.

The EBNs have four to six primary dendrites (mean = 5.2). The axon in some cases originates as a branch of a proximal dendrite, but in most neurons (76%) it emerges directly from the soma. The axon most often emerges ventrally (e.g., Fig. 11B,C [cf. 10B], 11D[cf. 10A]); it may also emerge dorsally (particularly in the more ventrally located neurons; see Fig. 7), laterally, or medially.

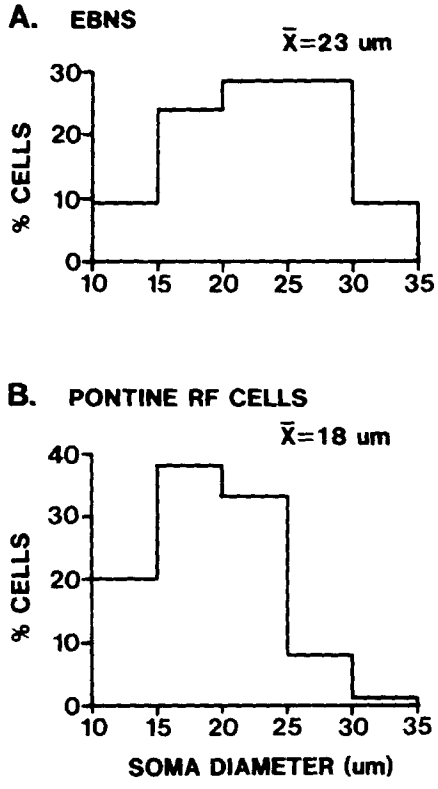

Fig. 9. Histograms of soma diameter. A. EBNs. B. Pontine reticular neurons retrogradely labelled with HRP from the ipsilateral abducens nucleus (represented by large dots in Fig. 8E-G).

Somatodendritic reconstructions of four EBNs are illustrated in Figure 11. The neurons have sparse dendritic arborizations, in which a relatively small number of primary dendrites give rise in turn to a small number of fairly straight and sparsely ramified secondary and tertiary dendrites. In these respects they appear to be typical of neurons in these regions of the reticular formation (Valverde, '61; Leontovich and Zhukova, '63; Ramon-Moliner and Nauta, '66). The neurons also exhibit the radiate or isodendritic branching pattern characteristic of reticular formation neurons (Ramon-Moliner and Nauta, '66) in that most of the daughter branches are longer than the parent branch from which they originate. The majority of primary dendrites branch within 60 μm of the soma; others extend for longer distances before branching, or extend unbranched, for distances of up to 800 μm, to their terminations.

The dendritic territories of the neurons in Figure 11 have a predominantly coronal orientation, with the dorsoventral and mediolateral extents exceeding the rostrocaudal extent. There is no preferred dendritic orientation within the coronal plane. The dendritic territories are contained primarily within the reticular formation and are strictly ipsilateral. Medially directed dendrites in some cases approach within 100 μm of the midline (Fig. 11A,C,D). Dorsal dendrites of some neurons extend into the MLF (e.g., Fig. 11A,C).

The EBNs shown in Figure 11 are in the reticular formation 80–1,100 μm rostral to the abducens. The most rostral of the EBNs in this study is shown in Figure 11A giving rise to an axon collateral (open arrowhead) that arborizes in the reticular formation rostral to the abducens. This collateral is generally found on the more rostral EBNs. In no case does this arborization extend into the neuron's dendritic field.

The neuron in Figure 11B is one of the most lateral, and also one of the most caudal of the EBNs, being located immediately rostral to the abducens. The ventral and lateral branches of this neuron's dendritic tree extend caudally into the rostral part of the abducens (not illustrated). The broken line in Figure 11B outlines the location of a fairly dense cellular region that appears as a dorsal extension of the reticular formation into the lateral part of the MLF. This dorsal cell group is present immediately rostral to the rostral border of the abducens and extends rostrally for approximately 800μm. It provides a consistent cytoarchitectural landmark through most of the rostrocaudal extent of the EBN region, although the EBNs are primarily ventral to this cell group. This cell group has been described as the dorsal paramedian pontine reticular formation and has been identified as receiving a projection from vestibular neurons with horizontal eye movement sensitivity (McCrea et al., '86b).

Axonal projections

EBN axons descend in the dorsal half of the reticular formation, usually 200–800 μm from the midline, giving off collaterals that arborize within specific regions of the reticular formation or course dorsally to enter and arborize in the abducens, the prepositus, or the medial part of the medial vestibular nucleus (MVN). Some collaterals to the abducens exit the nucleus caudally to terminate in the rostral MVN, immediately caudal to the abducens (e.g., Figs. 13, 16A).

Every EBN projects to the abducens, as well as to the IBN region of the reticular formation, ventral and caudal to the abducens (see Strassman et al., '86). Almost every EBN also projects to the prepositus (18/20, 90%) and the MVN (18/20, 90%), but there are no projections to other regions of the vestibular nuclei. Half of the EBNs project to the pontine reticular formation rostral to the abducens (e.g., Fig. 11A, 16A, top of Fig. 15). The axonal course and projection sites of all EBNs are strictly ipsilateral.

One EBN gives rise to a rostral collateral that ascends to the midbrain in the ventrolateral part of the MLF to arborize in the trochlear and oculomotor nuclei (this neuron is represented by a filled arrowhead in Fig. 4); this collateral could not be followed to its rostral limit. In all other cases, the rostralmost projections of EBNs are confined to the more caudal regions of the pontine reticular formation.

After descending to the caudal limit of its course, the main axon usually enters the prepositus and turns back rostrally (e.g., Figs. 13, 16B), in some cases ascending as far as the abducens. Neither the main axon nor any of its collaterals ever extends caudally beyond the caudal border of the prepositus. The axon and collaterals of EBNs remain within 2 mm of the midline, in no cases coursing further laterally than the lateral borders of the abducens or the MVN.

Figure 12 illustrates part of the axonal arborization of an EBN in the right nucleus prepositus. (A portion of this arborization is also shown in Fig. 10C.) A major axon collateral is shown entering the nucleus ventrally and taking a

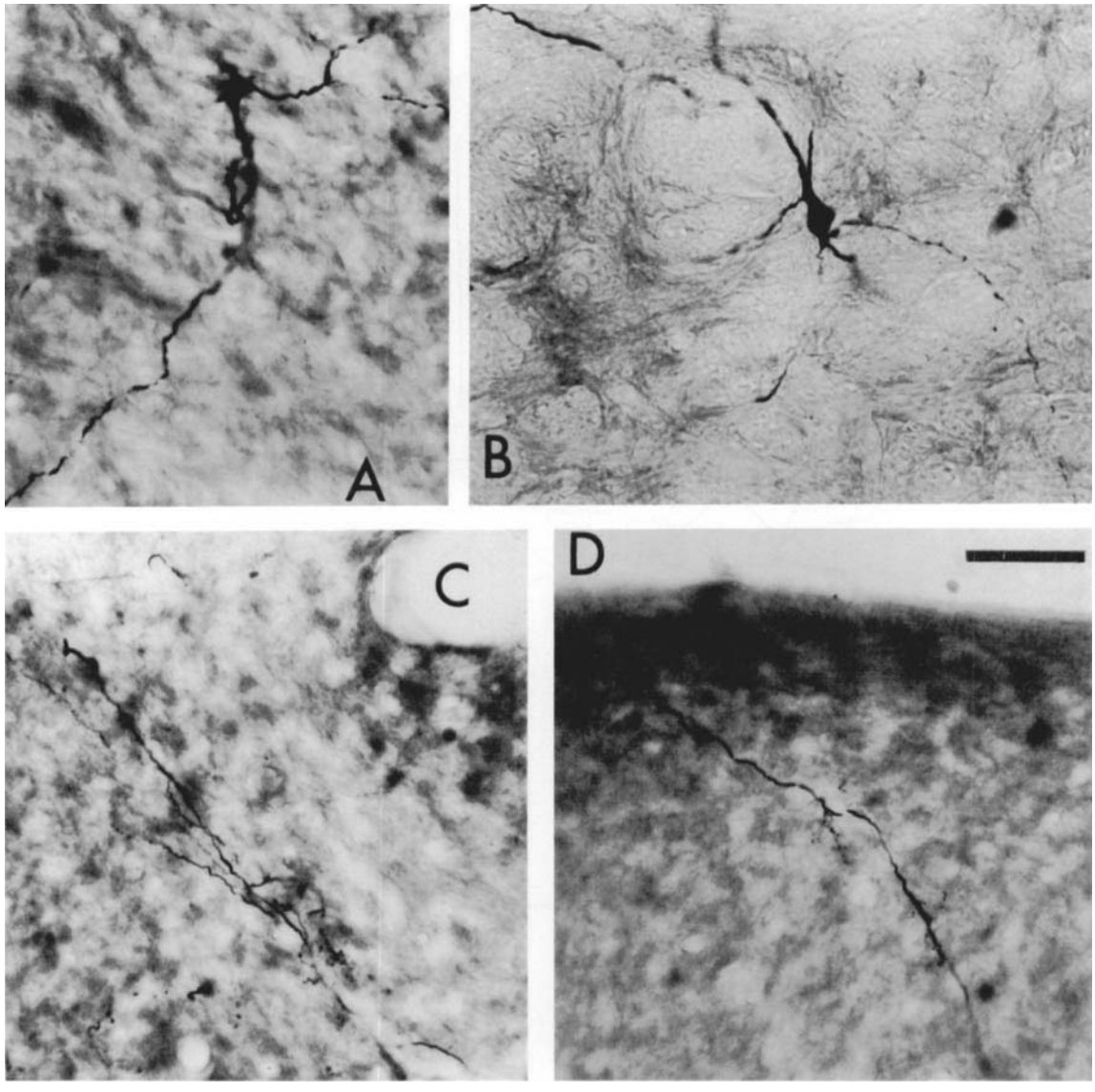

Fig. 10. A. EBN in the left reticular formation rostral to the abducen; reconstruction is shown in Figure 11D. B. EBN in the right reticular formation rostral to the abducens; reconstruction is shown in Figure 11C. C. Portion of an EBN arborization in the right nucleus prepositus; reconstruction is shown in Figure 12. D. Portion of an EBN arborization in the right abducens nucleus. Calibration = 50 μm for A–D.

circular course inside the dorsal, lateral, and ventral borders of the nucleus. It gives rises to finer collaterals that arborize throughout the nucleus. The arborization extends laterally to the border region between the prepositus and the MVN but does not extend further laterally into the MVN. The heavy projection to the prepositus and the border region with the MVN is typical of EBNs.

The axonal trajectory of an EBN with a more extensive projection to the MVN is illustrated on three coronal sections in Figure 13. Circles and triangles indicate the points at which an axon or collateral passes onto the caudally or rostrally adjacent section, respectively. (Rostral circles connect to caudal triangles.) The soma is shown in the rostral coronal section at the top of Figure 13, in the pontine reticular formation rostral to the abducens. (A more complete dendritic reconstruction of this neuron is shown in Fig. 11C.) The axon courses caudally into the ventromedial abducens (middle section) and gives off two major collaterals that arborize throughout the nucleus. The main axon continues caudally through the ventromedial abducens and into the dorsomedial part of the reticular formation (lower section), where it gives rise to a sparse arborization. It then turns dorsally to arborize heavily in the prepositus and the medial part of the MVN. Four other axonal branches that pass through the abducens also continue caudally onto the lower section (marked with open circles on the middle sec-

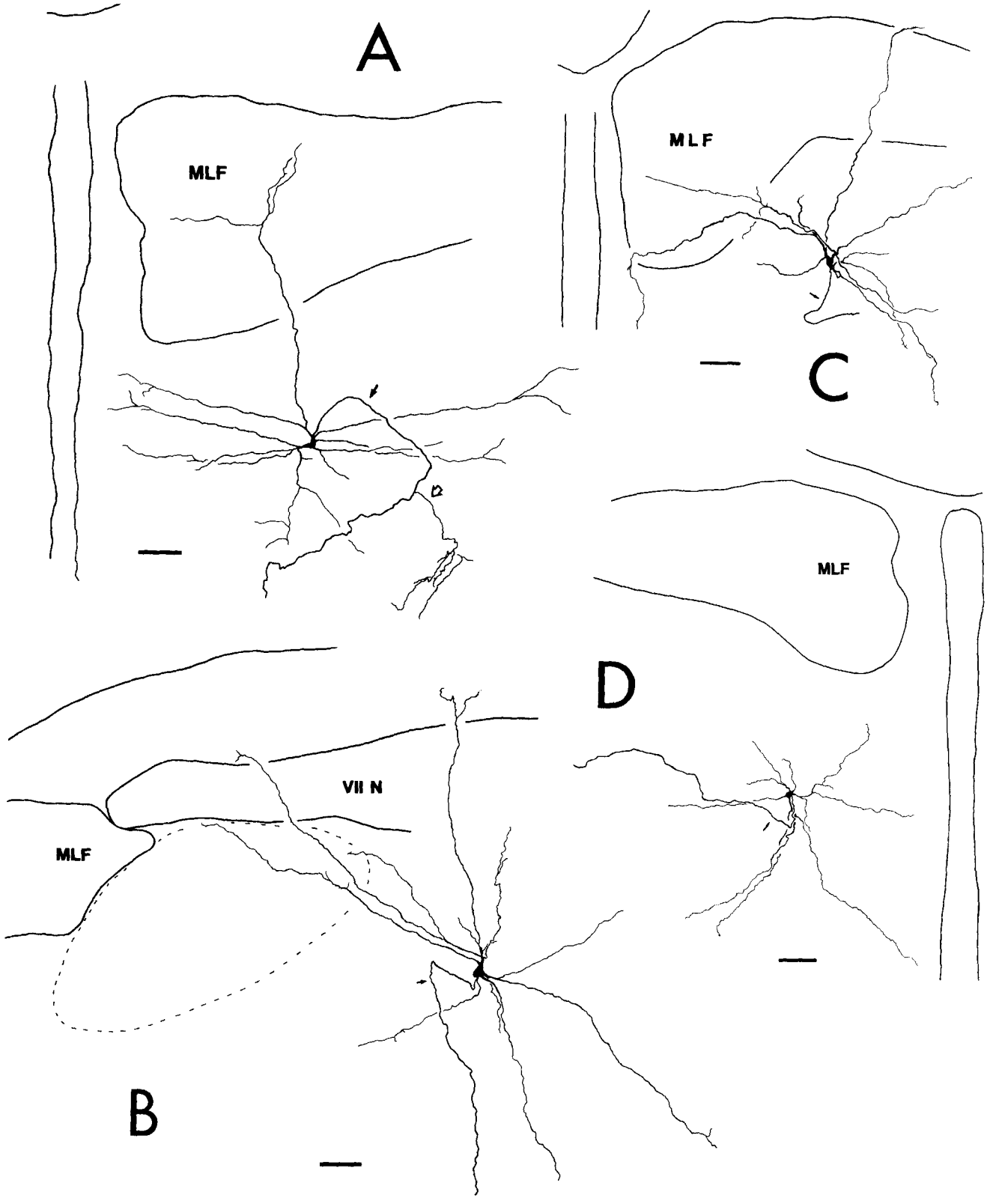

Fig. 11. Coronal soma-dendritic reconstructions of EBNs. Axons are indicated by arrows. The arrowhead in A points to an axon collateral in the reticular formation. The dashed lines in B show the location of a dorsal cell group in the caudal pontine reticular formation, described in the text. Calibration = 100 μm for A–D.

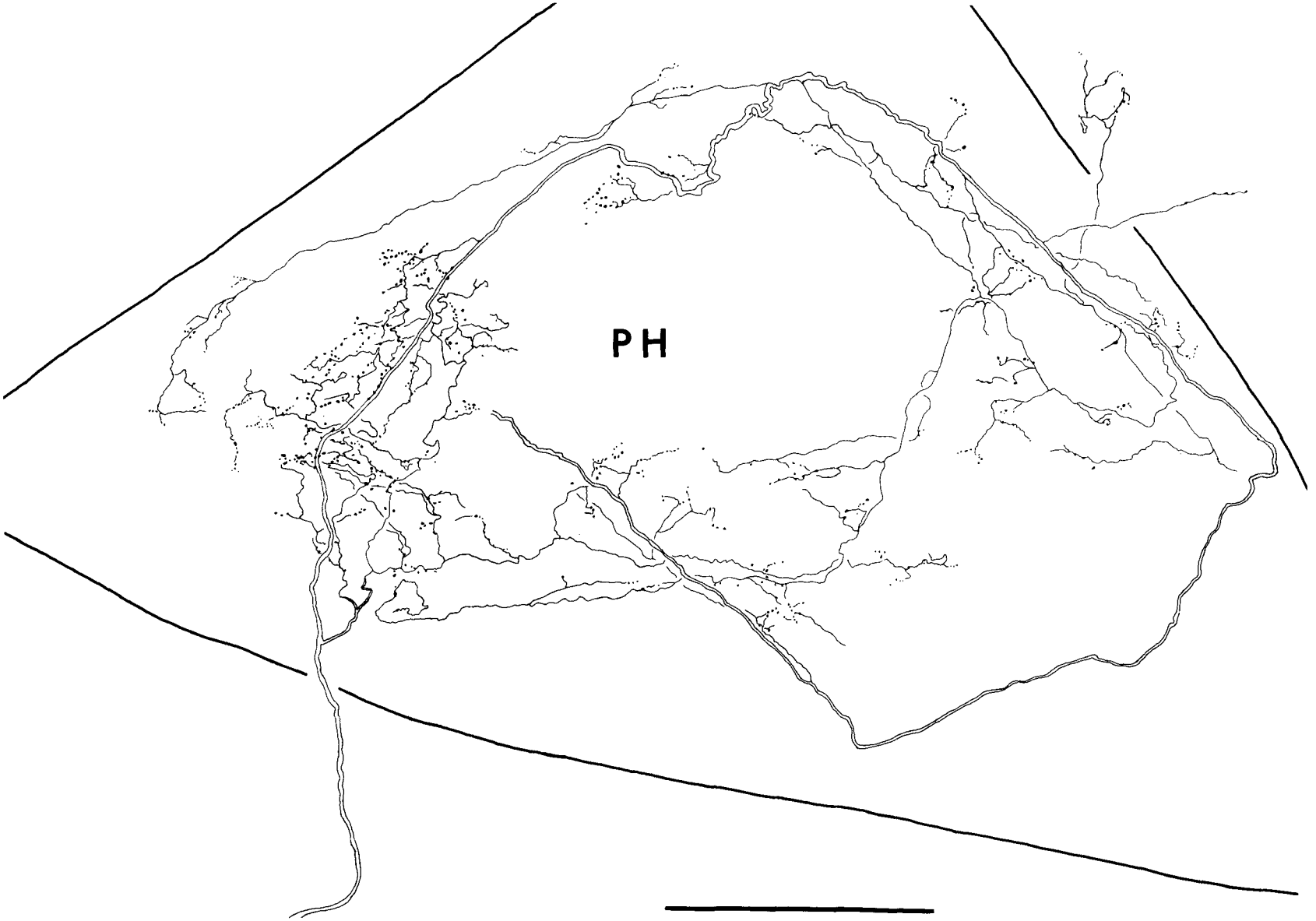

Fig. 12. Coronal reconstruction of the axonal arborization of an EBN in the right nucleus prepositus. Calibration = 200 μm.

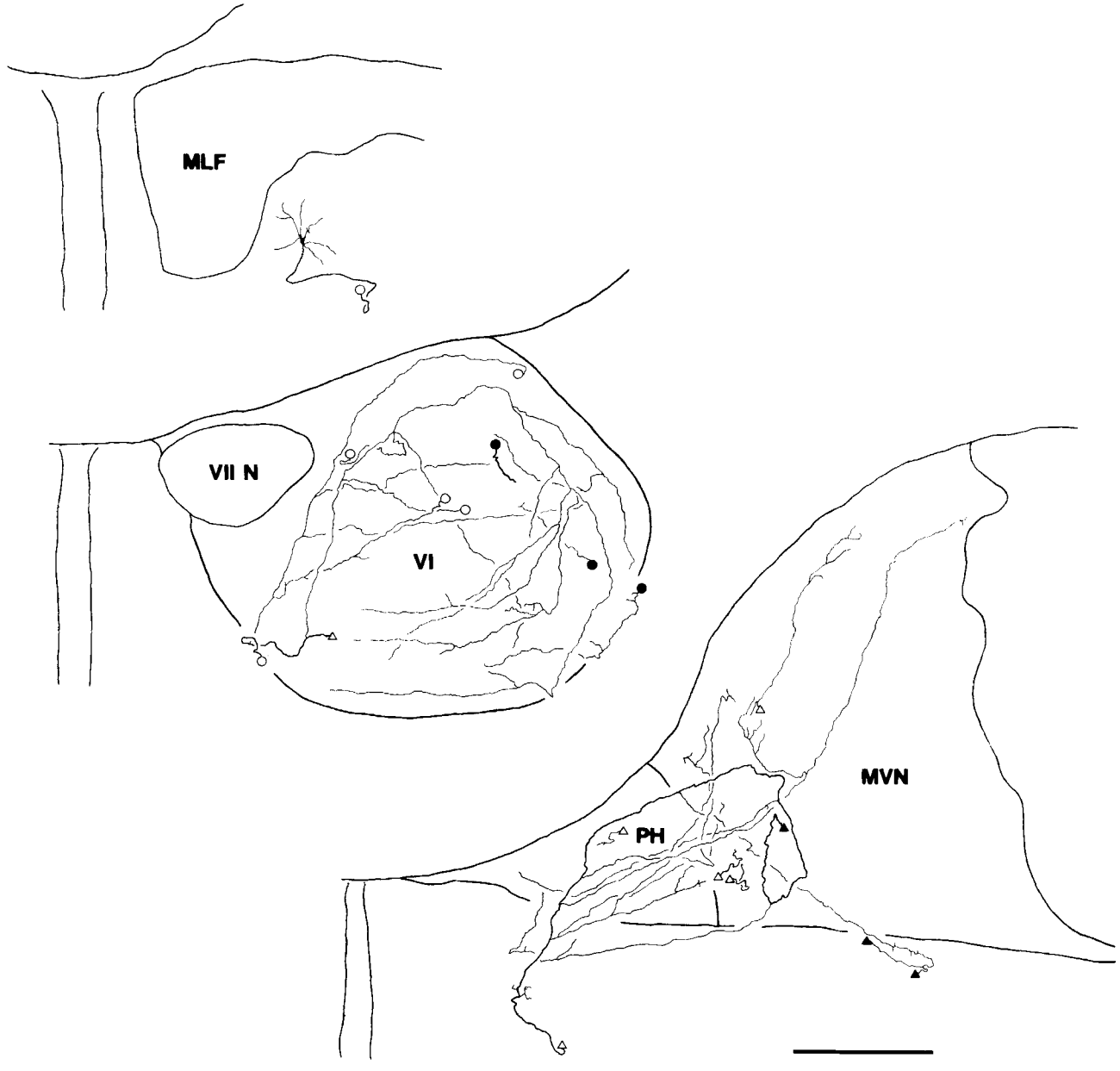

Fig. 13. Reconstruction of the full axonal trajectory of an EBN on three coronal sections. Circles and triangles mark the points at which axonal branches pass onto the caudally or rostrally adjacent section, respectively. Filled circles in the middle section and filled triangles in the bottom section mark points at which the main axon and two collaterals course rostrally to reenter the abducens. Calibration = 500 μm.

tion and open triangles on the lower section) and contribute to the arborization in the prepositus and the MVN. Two axonal branches course laterally through the MVN and arborize in the dorsolateral part of the nucleus. However, the heaviest part of the projection to the MVN is confined to the medial part of the nucleus, as is the case for most EBNs.

As shown on the lower section, the main axon courses laterally through the prepositus into the MVN. At this point it turns rostrally, along with two branches in the ventral MVN, and ascends into the abducens (marked with filled triangles on the lower section and filled circles on the middle section). The main axon of more than half of the EBNs turns rostrally in the prepositus, the MVN, or the underlying reticular formation and ascends a variable distance before terminating.

The regions of termination in the abducens nucleus of one EBN are illustrated in Figure 14 on a series of nine coronal sections. Although the terminations of a single neuron tend to be grouped in discrete patches, the EBN population as a whole projects to all regions of the nucleus (Fig. 17C,D). No relationship could be discerned between the pattern of termination in the abducens and the on-direction of saccadic sensitivity of each neuron.

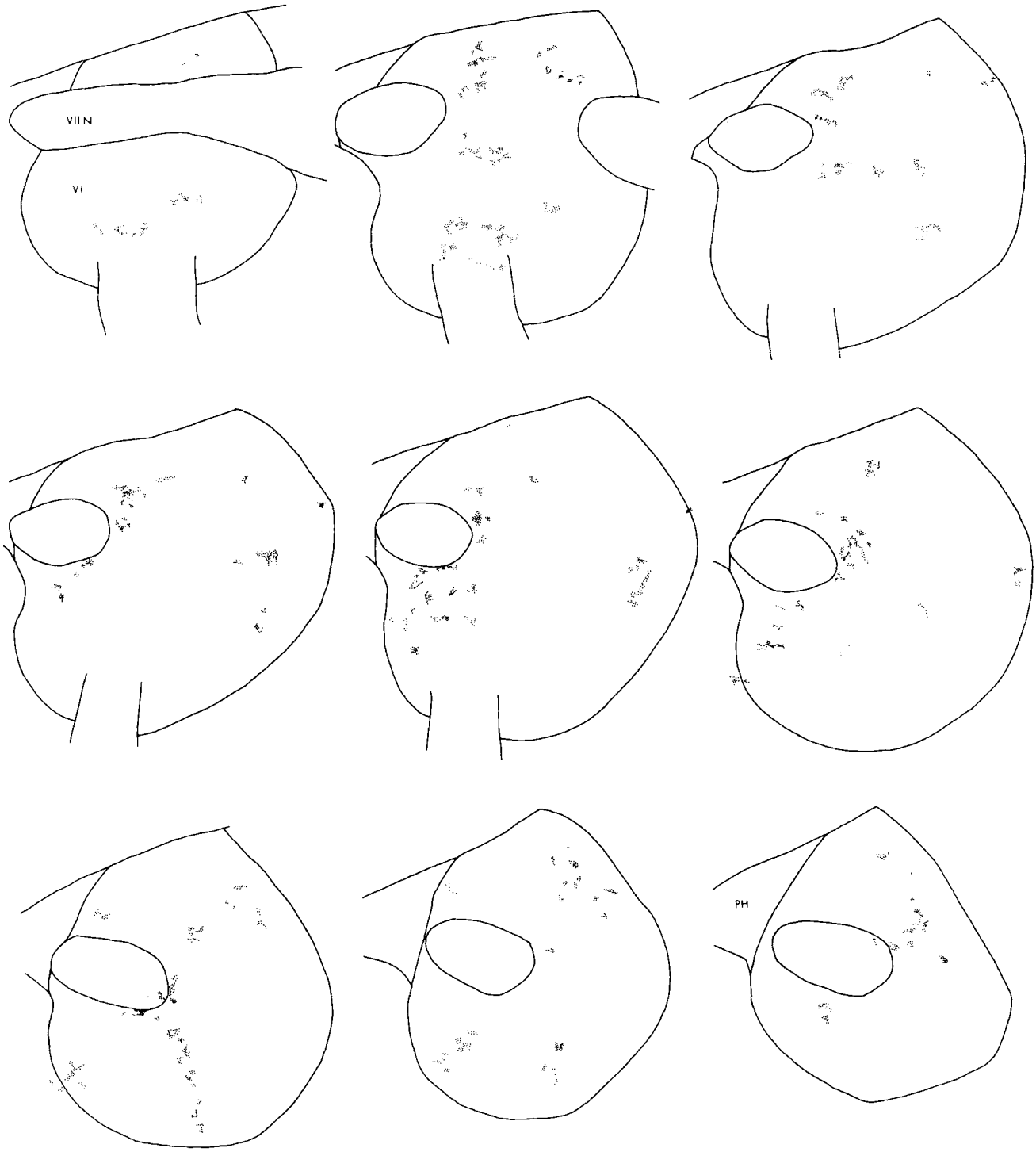

Fig. 14. Terminations of one EBN in the right abducens nucleus on nine coronal sections. The sections proceed caudally from left to right, starting at the upper left. Each dot represents a single bouton. The terminations from two adjacent 80-μm sections are represented on each section in the figure. Approximately 2,100 boutons are represented.

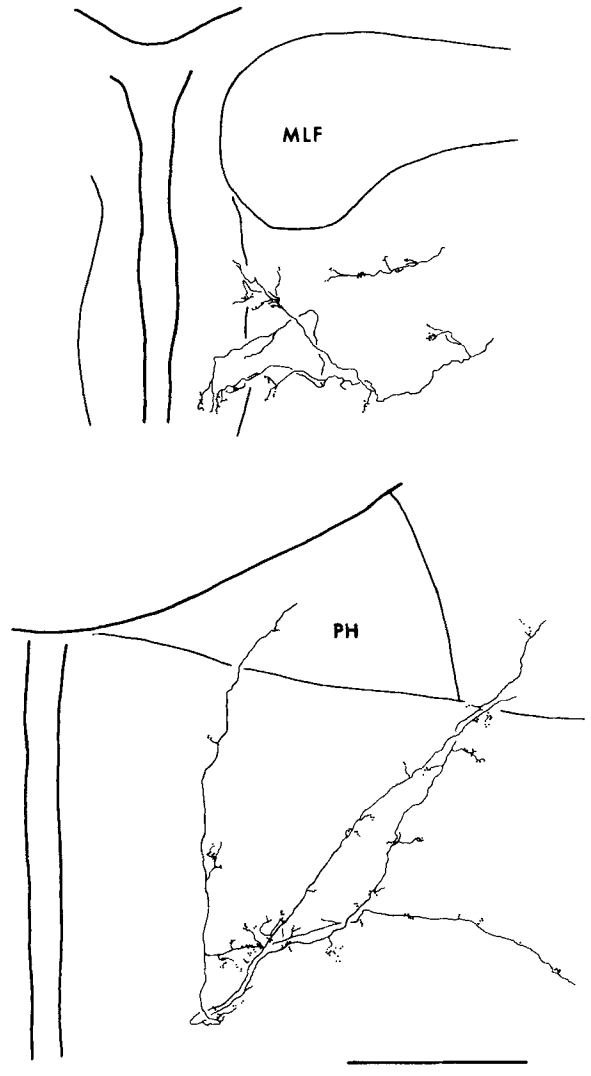

Fig. 15. Reconstructions of EBN axonal arborizations in the reticular formation on two coronal sections. Two EBN axons are shown in the upper section in the pontine reticular formation; one axon is shown in the lower section in the medullary reticular formation. Calibration = 500 μm.

Examples of arborizations in the reticular formation are illustrated on two coronal sections in Figure 15 for two EBN axons rostral to the abducens (top section) and one EBN axon caudal to the abducens (bottom section). EBN projections to the reticular formation rostral to the abducens often extend medially into the raphe (top section).

Two EBNs have a sparse projection to the nucleus of Roller, at the level of the caudal border of the prepositus (see Fig. 17H).

Figure 16 diagrams the projections of two EBNs on horizontal maps of the brainstem. Filled circles represent regions of termination in the abducens, the prepositus, and the MVN; open circles represent terminations in the reticular formation ventral to these nuclei. The figure illustrates the variability among EBNs in their pattern of projections. The neuron in Figure 16A has a heavy projection to the abducens and the adjacent part of the MVN, and a sparse projection to the prepositus. Also shown are projections to regions of the reticular formation both rostral and caudal to the abducens. In contrast, the neuron in Figure 16B has a lighter projection to the abducens but shows an extremely dense terminal arborization in the prepositus.

Figure 17 summarizes the regions of termination for the entire population of EBNs on a series of eight coronal sections. Heavy projections are present in the abducens nucleus (C,D), the nucleus prepositus (E–G), the MVN (E–G), and the IBN region of the reticular formation ventral and caudal to the abducens (D–F). The projection to the MVN is concentrated in the medial part of the nucleus. Lighter projections are present in the lateral part of the MVN, in the reticular formation rostral to the abducens (A,B), and in the nucleus of Roller (H). (Also see Figs. 17A,18A of Strassman et al., '86.)

DISCUSSION

The present study is the first to characterize the EBNs with intracellular staining, as well as the first to examine the firing of identified EBNs in relation to saccade parameters in the alert animal. The present results confirm the presence of a burst neuron population in the monkey analogous to the EBNs described previously in the cat (Igusa et al., '80; Sasaki and Shimazu, '81). Although there is no direct electrophysiological evidence in the monkey demonstrating the synaptic actions of burst neurons on motoneurons, an excitatory action is strongly indicated for the neurons in this study because their on-direction (ipsilateral) is the same as that of their target neurons in the abducens nucleus, and because they show a close anatomical and physiological correspondence to the EBNs in the cat.

Soma locations

The EBNs found in this study are restricted to the caudal part of the pontine reticular formation, immediately rostral to the abducens. Horizontal burst neurons have been found previously in the rostral part of the pontine reticular formation as well (Luschei and Fuchs, '72; Keller, '74; Kaneko et al., '81). More rostrally located neurons would be more difficult to label retrogradely from the intraaxonal injection sites near the abducens used in the present study. However, extracellular retrograde labelling indicates that the projection to the abducens from the pontine reticular formation arises primarily from the caudal part of this region (Fig. 8). Furthermore, studies using extracellular recording and antidromic stimulation, which have no limitations in demonstrating connections over long distances, have demonstrated a similar caudal distribution in the pontine reticular formation of burst neurons projecting to the ipsilateral abducens nucleus (Igusa et al., '80; Sasaki and Shimazu, '81). Possibly the more rostral burst neurons recorded in other studies lack a direct projection to abducens. This would be consistent with a report that in the monkey most of the burst neurons in the rostral pons do not show the close relationship to saccade parameters expected of neurons supplying a direct input to motoneurons (Hepp and Henn, '83).

Projections

Previous anterograde studies of the pontine reticular formation in the cat (Graybiel, '77) and monkey (Büttner-Ennever and Henn, '76) demonstrated ipsilateral projections to all of the regions found to receive EBN projections in the present study; these include the abducens, the pre-

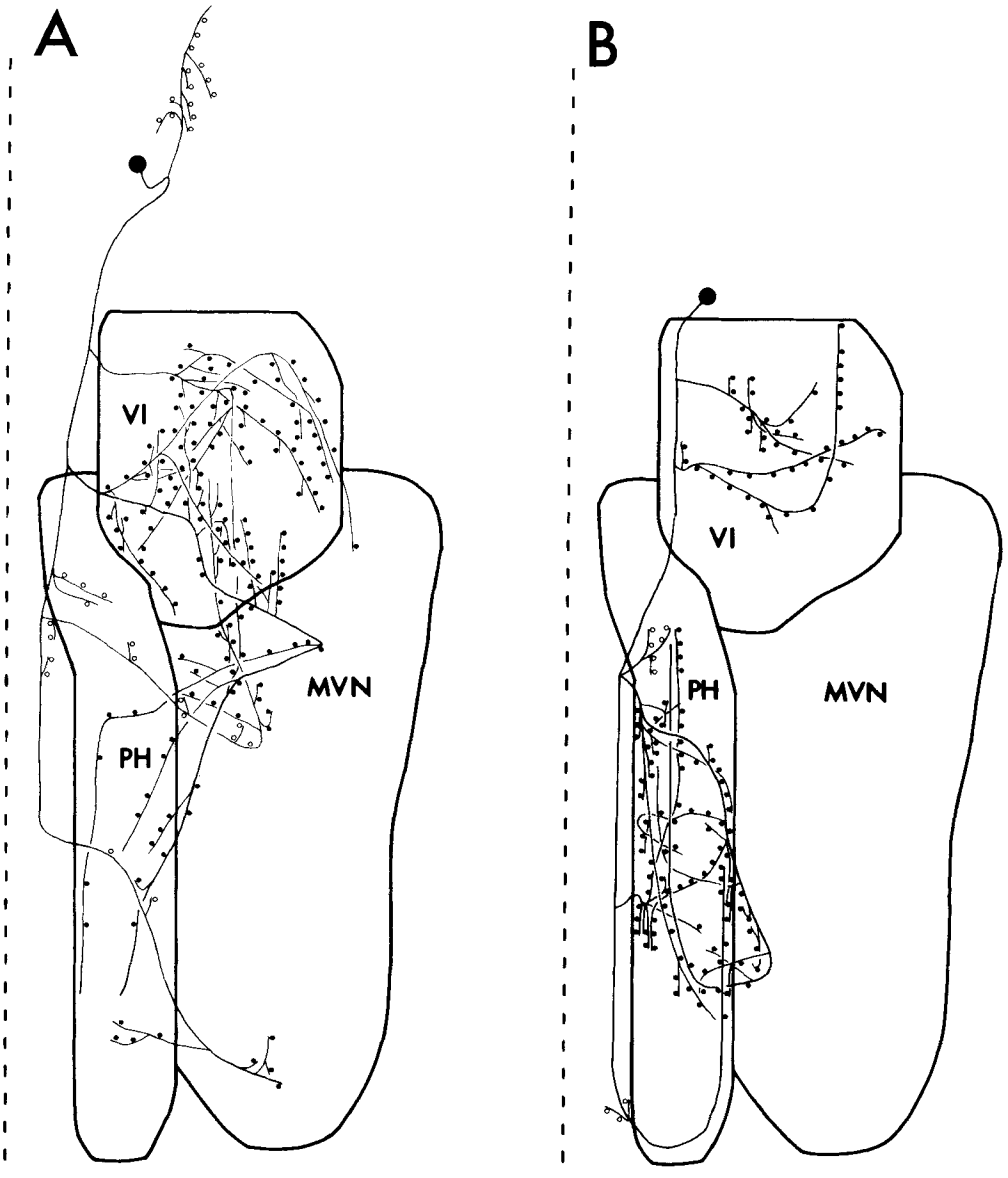

Fig. 16. Diagrams of two EBNs on horizontal maps of the brainstem. Filled circles mark regions in the abducens, the prepositus, and the MVN containing axonal boutons; open circles indicate regions containing boutons in the reticular formation ventral to these nuclei. The dashed line represents the midline on each section.

positus, the MVN, and the medullary reticular formation. These anterograde studies in additon found a major projection to the nucleus intercalatus, presumably arising from other classes of neurons present in this region of the reticular formation.

A previous study of EBNs in the cat found a similar pattern of projections on the basis of extracellular recording and mapping of low-threshold antidromic microstimulation sites (Sasaki and Shimazu, '81); axonal branching was demonstrated in the abducens, the MVN, and the IBN region of the reticular formation, ventral and caudal to the abducens. In addition, a class of neurons was found in the same region as the EBNs with projections to the spinal cord as well as the abducens, but with no saccadic modulation. An anatomically similar group of spinal-cord-projecting neurons has also been identified with intracellular staining (Grantyn et al., '80). However, no study of physiologically identified saccadic burst neurons has found a projection further caudally than the prepositus.

Physiological significance

The EBNs in this study have a saccadic modulation that is similar to that found previously for medium-lead burst neurons in the pontine reticular formation (Luschei and Fuchs, '72; Cohen and Henn, '72; Keller, '74; van Gisbergen et al., '81; Kaneko et al., '81) and is consistent with a major

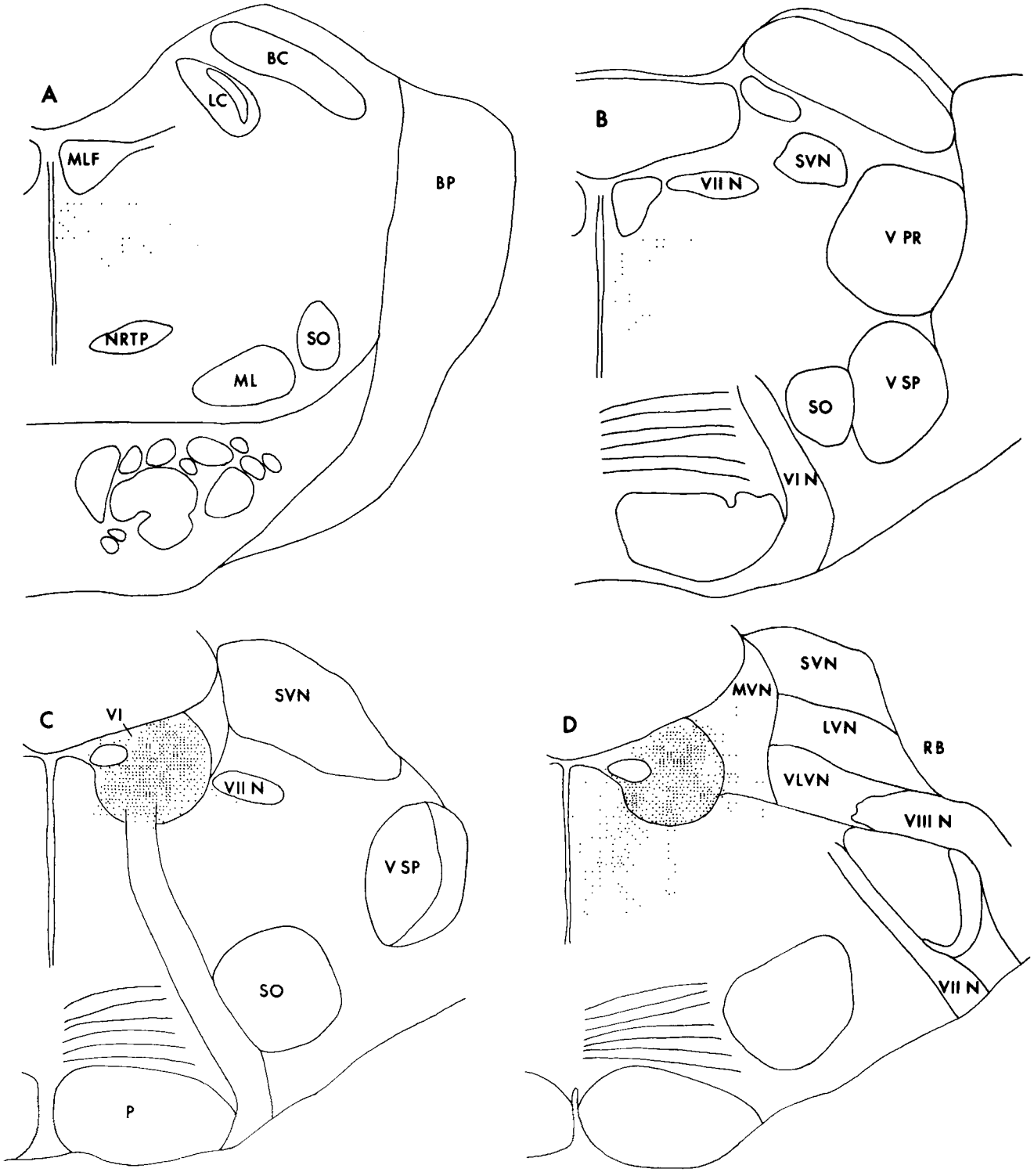

Fig. 17. Summary of EBN projections on eight coronal sections. The sections proceed caudally from A to H and are separated by 600–800 μm. The density of dots in each region represents the density of terminations for the entire population of EBNs.

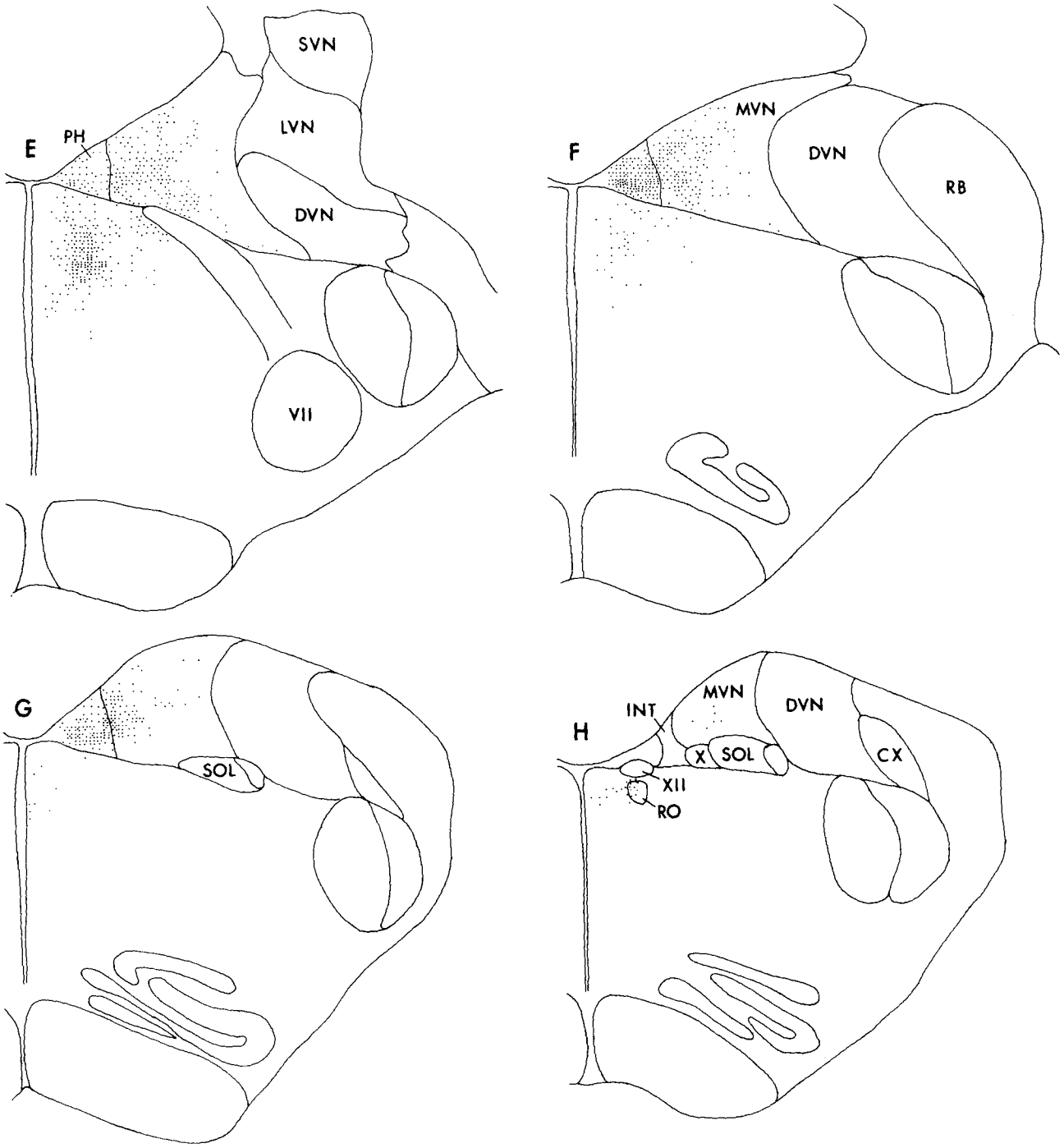

Figure 17 (cont'd)

role for these neurons in generating the burst in abducens motoneurons during ipsilateral saccades. The neurons show strong correlations between burst duration and saccade duration and between burst size and saccade amplitude, as is also found for motoneurons. The latencies of most of the neurons are comparable to those of neurons described as medium-lead in previous studies.

The EBN population as a whole has the horizontal on-direction consistent with its proposed role of supplying the primary excitatory saccadic drive to abducens motoneurons and internuclear neurons. However, individual neurons have on-directions with substantial vertical components, either upward or downward, that cannot be accounted for solely on the basis of their projection to the abducens. These oblique on-directions suggest that the saccadic signal driving the EBNs originates in neurons that also provide the input to the burst neuron populations that project to the oculomotor and trochlear nuclei. Such projections to EBNs could arise from long-lead burst neurons in the intermediate and deep layers of the superior colliculus, which may project to medium-lead burst neurons via long-lead burst neurons in the pontine reticular formation (Raybourn and Keller, '77; Keller, '79). The populations of long-lead burst neurons in the superior colliculus and pontine reticular formation code for the full range of saccade vectors, which must be reorganized into the single muscle vectors represented in each motoneuron pool (e.g., Henn and Cohen, '73). One way this might be accomplished is by an appropriate weighting in the projections of each long-lead burst neuron to the different medium-lead burst neuron populations controlling the various motoneuron pools (e.g., Fig. 1 of Sparks and Mays, '81). Such an arrangement implies that each medium-lead burst neuron, regardless of the specific motoneuron pool it projects to, receives a saccadic signal that originates in collicular burst neurons coding a wide range of saccade vectors. Figure 4 shows that the directional transformation of the colliculus's saccadic command is not yet complete at the level of the immediate premotor neurons. The final emergence of a purely horizontal saccadic signal apparently results from a summation of inputs from burst neurons (both EBNs and IBNs) with equal upward and downward components onto each abducens motoneuron. (The *temporal* transformation of the colliculus's saccadic signal (see Hepp and Henn, '83) is, however, essentially complete, as seen in the burst neurons' high correlation between burst duration and saccade duration.)

The oblique on-directions found in some EBNs suggest that these neurons may contribute to the saccadic firing of motoneurons in the oculomoter and trochlear nuclei. Although all but one of the EBNs lack direct projections to these nuclei, most of the neurons have a major projection to the prepositus, which projects to all three extraocular motor nuclei (McCrea and Baker, '85) and has eye-movement-related neurons with a wide range of on-directions (Baker et al., '75; Lopez-Barneo et al., '82). Thus, the range of EBN on-directions shown in Figure 4 could be explained both by a convergence of projections to EBNs from long-lead burst neurons with a range of directional selectivities and by a divergence of EBN projections to multiple motor and premotor pathways.

The physiological properties and projections of EBNs will be discussed further and compared with the IBNs in the following paper (Strassman et al., '86).

LITERATURE CITED

Adams, J.C. (1981) Heavy metal intensification of DAB-based HRP reaction product. J. Histochem. Cytochem. *29*:775.

Baker, R., M. Gresty, and A. Berthoz (1975) Neuronal activity in the prepositus hypoglossi nucleus correlated with vertical and horizontal eye movement in the cat. Brain Res. *101*:366–371.

Brodal, A. (1957) The Reticular Formation of the Brain Stem of the Cat: Anatomical Aspects and Functional Correlations. London: Oliver and Boyd.

Büttner-Ennever, J.A., and V. Henn (1976) An autoradiographic study of the pathways from the pontine reticular formation involved in horizontal eye movements. Brain Res. *108*:155–164.

Carpenter, R.H.S. (1977) Movements of the Eyes. London: Pion.

Cohen, B., and A. Komatsuzaki (1972) Eye movements induced by stimulation of the pontine reticular formation: Evidence for integration in oculomotor pathways. Exp. Neurol. *36*:101–117.

Cohen, B., A. Komatsuzaki, and M.B. Bender (1968) Electrooculographic syndrome in monkeys after pontine reticular formation lesions. Arch. Neurol. *18*:78–92.

Cohen, B., and V. Henn (1972) Unit activity in the pontine reticular formation associated with eye movements. Brain Res. *46*:403–410.

Collins, C.C., D. O'Meara, and A.B. Scott (1975) Muscle tension during unrestrained human eye movements. J. Physiol. (Lond.) *245*:351–369.

Delgado-Garcia, J., R. Baker, and S.M. Highstein (1977) The activity of internuclear neurons identified within the abducens nucleus of the alert cat. In R. Baker and A. Berthoz (eds): Control of Gaze by Brain Stem Neurons, Developments in Neuroscience, Vol. 1. New York:Elsevier/North-Holland, pp.291–301.

Dodge, R. (1903) Five types of eye movements in the horizontal meridian plane of the field of regard. Am. J. Physiol. *8*:307.

Fuchs, A.F., and E.S. Luschei (1970) Firing patterns of abducens neurons of alert monkeys in relationship to horizontal eye movement. J. Neurophysiol. *33*:382–392.

Gacek, R.R. (1979) Location of abducens afferent neurons in the cat. Exp. Neurol. *64*:342–353.

Goldstein, H.P. (1983) The Neural Encoding of Saccades in the Rhesus Monkey. Ph.D. Thesis, Johns Hopkins University.

Granytn, R., R. Baker, and A. Grantyn (1980) Morphological and physiological identification of excitatory pontine reticular neurons projecting to the cat abducens nucleus and spinal cord. Brain Res. *198*:221–228.

Graybiel, A.M. (1977) Direct and indirect preoculomotor pathways of the brainstem: An autoradiographic study of the pontine reticular formation in the cat. J. Comp. Neurol. *175*:37–78.

Graybiel, A.M., and E.A. Hartweig (1974) Some afferent connections of the oculomotor complex in the cat: an experimental study with tracer techniques. Brain Res. *81*:543–551.

Henn, V., and B. Cohen (1973) Quantitative analysis of activity in eye muscle motoneurons during saccadic eye movements and positions of fixations. J. Neurophysiol. *36*:115–126.

Henn, V., and B. Cohen (1976) Coding of information about rapid eye movements in the pontine reticular formation of alert monkeys. Brain Res. *108*:307–325.

Hepp, K., and V. Henn (1983) Spatio-temporal recording of rapid eye movement signals in the monkey paramedian pontine reticular formation (PPRF). Exp. Brain Res. *52*:105–120.

Highstein, S.M., and R. Baker (1978) Excitatory termination of abducens internuclear neurons on medial rectus motoneurons: Relationship to syndrome of internuclear opthalmoplegia. J. Neurophysiol. *41*:1647–1661.

Highstein, S.M., A. Karabelas, R. Baker, and R.A. McCrea (1982) Comparison of the morphology of physiologically identified abducens motor and internuclear neurons in the cat: A light microscopic study employing the intracellular injection of horseradish peroxidase. J. Comp. Neurol. *208*:369–381.

Hikosaka, O., and T. Kawakami (1977) Inhibitory neurons related to the quick phase of vestibular nystagmus—their location and projection. Exp. Brain Res. *27*:377–396.

Hikosaka, O., Y. Igusa, S. Nakao, and H. Shimazu (1978) Direct inhibitory synaptic linkage of pontomedullary reticular burst neurons with abducens motoneurons in the cat. Exp. Brain Res. *33*:337–352.

Hikosaka, O., Y. Igusa, and H. Imai (1980) Inhibitory connections of nystag-

mus-related reticular burst neurons with neurons in the abducens, prepositus hypoglossi and vestibular nuclei in the cat. Exp. Brain Res. *39:*301–311.

Igusa, Y., S. Sasaki, and H. Shimazu (1980) Excitatory premotor burst neurons in the cat pontine reticular formation related to the quick phase of vestibular nystagmus. Brain Res. *182:*451–456.

Judge, S.J., B.J. Richmond, and F.C. Chu (1980) Implantation of magnetic search coils for measurements of eye position: An improved method. Vision Res. *20:*535–8.

Kaneko, C.R.S., C. Evinger, and A.F. Fuchs (1981) Role of cat pontine burst neurons in generation of saccadic eye movements. J. Neurophysiol. *46:*387–408.

Keller, E.L. (1974) Participation of the medial pontine reticular formation in eye movement generation in monkey. J. Neurophysiol. *37:*316–332.

Keller, E.L. (1979) Colliculoreticular organization in the oculomotor system. In R. Granit and O. Pompeiano (eds): Reflex Control of Posture and Movement. Amsterdam: Elsevier, Prog. Brain Res. *50:*725–734.

King, W.M., S.G. Lisberger, and A.F. Fuchs (1976) Responses of fibers in medial longitudinal fasciculus (MLF) of alert monkeys during horizontal and vertical conjugate eye movements evoked by vestibular or visual stimuli. J. Neurophysiol. *39:*1135–1149.

Leontovich, T.A., and G.P. Zhukova (1963) The specificity of the neuronal structure and topography of the reticular formation in the brain and spinal cord of carnivora. J. Comp. Neurol. *121:*347–379.

Lopez-Barneo, J., C. Darlot, A. Berthoz, and R. Baker (1982) Neuronal activity in prepositus nucleus correlated with eye movement in the alert cat. J. Neurophysiol. *47:*329–352.

Luschei, E.S., and A.F. Fuchs (1972) Activity of brain stem neurons during eye movements of alert monkeys. J. Neurophysiol. *35:*445–461.

Maciewicz, R.J., K. Eagen, C.R.S. Kaneko, and S. Highstein (1977) Vestibular and medullary brain stem afferents to the abducens nucleus in the cat. Brain Res. *123:*229–240.

McCrea, R.A., and R. Baker (1985) Anatomical connections of the nucleus prepositus of the cat. J. Comp. Neurol. *237:*377–407.

McCrea, R.A., K. Yoshida, A. Berthoz, and R. Baker (1980) Eye movement related activity and morphology of second order vestibular neurons terminating in the cat abducens nucleus. Exp. Brain Res. *40:*468–473.

McCrea, R.A., A. Strassman, and S.M. Highstein (1986a) Morphology and physiology of abducens motoneurons and internuclear neurons intracellularly injected with horseradish peroxidase in alert squirrel monkeys. J. Comp. Neurol. *243:*291–308.

McCrea, R.A., A. Strassman, E. May, and S.M. Highstein (1986b) Anatomical and physiological characteristics of vestibular neurons mediating the horizontal vestibuloocular reflex in the squirrel monkey. J. Comp. Neurol. (submitted).

Mesulam, M.-M. (1978) Tetramethyl benzidine for horseradish peroxidase neurohistochemistry: A noncarcinogenic blue reaction product with superior sensitivity for visualizing neural afferents and efferents. J. Histochem. Cytochem. *26:*106–117.

Olszewski, J., and D. Baxter (1954) Cytoarchitecture of the Human Brain Stem. Basel:J.B. Lippincott Co.

Pola, J., and D.A. Robinson (1978) Oculomotor signals in medial longitudinal fasciculus of the monkey. J. Neurophysiol. *41:*245–259.

Ramon-Moliner, E., and W.J.H. Nauta (1966) The isodendritic core of the brain stem. J. Comp. Neurol. *126:*311–336.

Raybourn, M.S., and E.L. Keller (1977) Colliculoreticular organization in primate oculomotor system. J. Neurophysiol. *40:*861–878.

Robinson, D.A. (1963) A method of measuring eye movement using a scleral search coil in a magnetic field. IEEE Trans. Biomed. Electron. *BME-10:*137–145.

Robinson, D.A. (1970) Oculomotor unit behavior in the monkey. J. Neurophysiol. *33:*393–404.

Robinson, D.A (1971) Models of oculomotor neural organization. In P. Bach-Y-Rita, C.C. Collins, and J.E. Hyde (eds): The Control of Eye Movements. New York: Academic Press, pp. 519–538.

Robinson, D.A. (1975) Oculomotor control signals. In P. Bach-Y-Rita and G. Lennerstrand (eds): Basic Mechanisms of Oculomotor Motility and Their Clinical Implications. Oxford: Pergamon Press, pp. 337–378.

Robinson, D.A., D.M. O'Meara, A.B. Scott, and C.C. Collins (1969) Mechanical components of human eye movements. J. Appl. Physiol. *26:*548–553.

Sasaki, S., and H. Shimazu (1981) Reticulovestibular organization participating in generation of horizontal fast eye movement. Ann. N.Y. Acad. Sci. *374:*130–143.

Schiller, P.H. (1970) The discharge characteristics of single units in the oculomotor and abducens nuclei of the unanesthetized monkey. Exp. Brain Res. *10:*347–362.

Sparks, D.L., and L.E. Mays (1981) The role of the monkey superior colliculus in the control of saccadic eye movements: a current perspective. In A.F. Fuchs and W. Becker, (eds): Progress in Oculomotor Research, Developments in Neuroscience, Vol. 12.

Sparks, D.L., and R.P. Travis (1971) Firing pattern of reticular neurons during horizontal eye movements. Brain Res. *33:*477–481.

Steiger, H.-J., and J.A. Büttner-Ennever (1978) Relationship between motoneurons and internuclear neurons in the abducens nucleus: A double retrograde tracer study in the cat. Brain Res. *148:*181–188.

Steiger, H.-J., and J.A. Büttner-Ennever (1979) Oculomotor nucleus afferents in the monkey demonstrated with horseradish perixodase. Brain Res. *160:*1–15.

Strassman, A., S.M. Highstein, and R.A. McCrea (1986) Anatomy and physiology of saccadic burst neurons in the squirrel monkey. II. Inhibitory burst neurons. J. Comp. Neurol. *249:*358–380.

Taber, E. (1961) The cytoarchitecture of the brain stem of the cat I. Brain stem nuclei of the cat. J. Comp. Neurol. *116:*27–69.

Valverde, F. (1961) Reticular formation of the pons and medulla oblongata. A Golgi study. J. Comp. Neurol. *116:*71–99.

van Gisbergen, J.A.M., D.A. Robinson, and S. Gielen (1981) A quantitative analysis of generation of saccadic eye movements by burst neurons. J. Neurophysiol. *45:*417–442.

Yarbus, A.L. (1967) Eye Movements and Vision. New York: Plenum Press.

Yoshida, K., R.A. McCrea, A. Berthoz, and P.P. Vidal (1982) Morphological and physiological characteristics of inhibitory burst neurons controlling horizontal rapid eye movements in the alert cat. J. Neurophysiol. *48:*761–784.